Preparation and Characterization of Ring-based Polymers with Various Architectures and Their Viscoelastic Properties

Yuya DOI

TABLE OF CONTENS

Chapter 1
Introduction 1

1.1. General Introduction 1
1.2. Polymer Chain Dynamics 2
1.3. Ring-based Polymers with Various Architectures 6
1.4. Outline of This Thesis 7
1.5. References 9

Chapter 2
Preparation and Characterization of Ring-based Polymers with Various Architectures 13

2.1. Introduction 14
2.2. Experimental 15
2.3. Results and Discussion 21
2.4. Conclusions 33
2.5. References 33

Chapter 3
Viscoelastic Properties of Ring Polystyrenes with Ultrahigh Purity 34

3.1. Introduction 35
3.2. Experimental 36
3.3. Rheological Data Analyses 37
3.4. Results and Discussion 38
3.5. Conclusions 46
3.6. References 47

Chapter 4
Viscoelastic Properties of Tadpole-Shaped Polystyrenes 48

4.1. Introduction 49
4.2. Experimental 50
4.3. Results and Discussion 51
4.4. Conclusions 60
4.5 References 61

Chapter 5
Viscoelastic Properties of Comb-Shaped Ring Polystyrenes 62

5.1. Introduction 63
5.2. Experimental 64
5.3. Results and Discussion 65
5.4. Conclusions 69
5.5. References 69

Chapter 6
Viscoelastic Properties of Dumbbell-Shaped Polystyrenes 70

6.1. Introduction 71
6.2. Experimental 72
6.3. Results and Discussion 73
6.4. Conclusions 77
6.5. References 77

Chapter 7
Summary 78

List of Publications 80

Acknowledgements 81

Chapter 1

Introduction

1.1. General Introduction

Polymers or macromolecules can be divided into two major classes: natural and synthetic ones. Natural polymers such as rubber, wool, silk and cellulose, have been used since ancient times before they were recognized as long chain molecules. Protein and DNA, which constitute our human body, are also a family of the natural polymers. To the contrary, synthetic polymers such as nylons, polyesters, polyolefins and synthetic rubbers are generally transformed from petroleum oil. They have been normally produced on a huge scale and utilized in various fields today. Both natural and synthetic polymers play indispensable roles in a variety of fields of our daily life.

The properties of polymers are affected by various molecular factors, i.e., monomer species, chain length, its distribution, chain architecture, etc. Among them, chain architecture, namely the connectivity of monomers, is believed to greatly affect various physical properties of polymers, and they can be roughly classified into the following three types: linear, branched and ring molecules. Linear polymers possess the simplest structure with a continuous long flexible chain and their conformation can be representatively expressed by random coils. In general, their properties can give the fundamentals of all the polymer species.

Branched polymers are the molecules that have one or more branch points where side chains are attached to the main chain. They can be secondly categorized as star, graft, dendrimer, hyperbranched and cross-linked polymers according to their chain connectivity. Some

commercially available and extraordinary useful polymers such as polyolefin are made up of chains with complex branching, and their physical properties have been extensively studied until date.[1,2]

Ring polymers are in another category of non-linear type molecules and have a unique structural feature of possessing no chain ends on them. Some DNA and biomolecules are known to have circular architecture in nature,[3,4] while some polycondensation products synthesized by step-growth polymerization are also conceived to contain cyclic polymers.[5] Moreover, recent development of synthetic techniques enables us to prepare ring polymers strategically.[3,6-15] The absence of chain ends on ring molecules might generate some characteristic physical properties, which must be completely different from those of linear molecules. In fact, a large number of studies have been extensively pursued theoretically,[16-33] computationally[34-54] and experimentally[55-85] to date. However, their whole picture concering physical properties is still not quite clear, mainly because the samples used in the experiments are contaminated with several impurities, and therefore many studies are still on going.

1.2. Polymer Chain Dynamics

Polymer melts or concentrated solutions are known to exhibit complicated responses when several forces are applied on them; in a short time scale they behave as elastic solids, while in a long time scale they behave as viscous liquids. This complex property is known as "viscoelasticity", and is one of the most distinctive properties of polymers. It is closely related to the polymer chain motion, because one of the origins of viscoelasticity is anisotropy in chain

conformation generated by the deformation strain, and this anisotropy can be recovered by the chain motion.

Viscoelastic behavior of isolated short linear polymer melts was successfully described by Rouse.[86] In the Rouse model, a polymer chain is represented by using alternative beads and springs, which follow the Gaussian distribution statistics, and its viscoelastic response can be determined by the balance between entropy elasticity from springs and frictional force from beads.

For long linear polymer melts, their viscoelastic properties are known to be greatly different from those for the short ones. They exhibit plateaus in relaxation moduli within the region between the glass transitions and the terminals. Actual magnitude of each modulus is independent of the molecular weight of linear chains, while the length of plateau is extended with increase of the molecular weight. This long-time plateau is called "rubbery plateau" due to the analogous similarity to the cross-liked rubber, and is originated from entanglements of long linear chains. In entangled polymer systems, the reptation motion based on the tube model, which is proposed by de Gennes,[87] Doi and Edwards,[88] is widely applied to describe the chain motion. This model assumes that a polymer chain cannot across the other chains and can only diffuse along its contour to release the stress instead. By considering additional effects such as constraint release (CR) and contour length fluctuations (CLF), this reptation model has acquired the considerable success to describe the entangled polymer chain dynamics.[89-91]

Tube model can also describe the complex chain motion of entangled branched polymers by considering the effect of the branch points. For example, star polymers, which are regarded as the simplest class of branched polymers, cannot simply follow the reptation motion due to the

existence of the branch point. In contrast to the simple reptation, each arm can retract from the free chain ends to the branch point to relax.[87-91] Relaxation motion for more complicated branched molecules, such as combs and pom-pom type polymers can also be well described by the hierarchical relaxation using the tube models.[92]

To the contrary, tube models such as reptation or retraction motions cannot be simply adapted for ring polymers due to their inherent architectures with no chain ends. Several models were proposed to express the conformations and dynamics of ring molecules instead. For example, the Rouse bead-spring model can also be applied to the ring molecules, when they are in unentangled states and their conformations are admitted to follow the Gaussian chain distribution.[28,29,44] Moreover, the double-folded linear-like conformation[30] and the lattice-animal branched-like conformation[31-33] were adopted when their molecular weights are large enough to penetrate each other deeply. In 1980s, many experimental results for the rheological measurements for synthetic ring polymers were reported by Roovers[64,67] and McKenna,[65,70] however, comprehensive results were not obtained probably due to the lack of the samples with guaranteed ring purity.

Recently, several high performance liquid chromatography (HPLC) techniques such as liquid chromatography at the critical condition (LCCC) or interaction chromatography (IC) have been discovered and developed. These methods made it possible to separate ring chains from linear ones, and consequently the ring purity can be estimated accurately.[93,94]

By utilizing this LCCC method, Kapnistos et al. reported the remarkable viscoelastic properties of highly-purified two ring PS samples with their molecular weights M_w = 161 and 198 kg/mol, which are sufficiently larger than the entanglement molecular weight M_e (= 18.0 kg/mol) for linear PS.[77] They demonstrated two rings did not exhibit apparent rubbery plateaus but

represent power-law decay of the stress relaxation function. These results indicate that rings adopt completely different chain relaxation mechanisms from linear polymers, while they show some characteristic intermolecular interactions instead. However, only two ring samples in the same molecular weight range were treated in the report. Following their study, several experimental data on the ring dynamics were newly reported, but the whole picture of the ring chain motion has not been clarified yet.[78-85]

Not only the dynamics of ring homopolymers, but also that of the ring/linear blend systems must be an intriguing subject. Kapnistos et al. reported experimentally the influence of the linear contamination in the ring samples on their rheological responses.[77] They revealed that a tiny amount (only 0.07 %) of a long linear chain with about $10M_e$ which has the same molecular weight as the ring sample, sensitively caused a change in the rheological response, and furthermore revealed that the blend sample including 1% of the linear chain exhibited a plateau. Halverson et al. reported on the systematic change in the rheological response of ring/linear blends depending on their composition, where both ring and linear chains have the molecular weight of $10M_e$, by the molecular dynamics (MD) simulations,[49] they also demonstrated the evident viscosity increase due to the linear contaminations. Moreover, for the 50/50 ring/linear blend, its viscosity was confirmed to increase up to two times as large as that for the pure linear chain. These results might be considered to be caused by the new type of interactions i.e., ring-linear penetrations. To elucidate this mechanism, the dynamics of ring/linear blends has been kept studying.

In fact, the ring-linear penetration may be similar to the threading dynamics of polymers through confined spaces such as membranes and nanopores. This sort of phenomenon is well-known in DNA and biopolymer interactive systems,[95] while another example of ring-linear

penetration is inclusion complexes between cyclodextrins and guest polymers.[96,97] These systems may give us some clues to elucidate the ring-linear penetration mechanism.

1.3. Ring-based Polymers with Various Architectures

As explained above, the dynamics of ring polymers and ring/linear blends is attractive and intriguing. Then if ring and linear chains are introduced into one molecule, what kinds of viscoelastic properties can appear? The simplest example of this type of molecule is a "tadpole-shaped polymer", where a linear chain is attached on a ring, as schematically illustrated in Figure 1-1(b). This molecule is expected to generate intermolecular ring-linear penetrations easily and to exhibit further synergistic viscoelastic properties due to the connectivity of a ring and a linear chain. Moreover, in the case of a "comb-shaped ring polymer", where multiple linear chains are attached on a ring, as shown in Figure 1-1(c), the effectiveness of the ring-linear penetration might increase. In contrast, in the case of a "dumbbell-shaped polymer" as drawn in Figure 1-1(d), where rings are attached on both ends of a linear chain, its viscoelastic properties are also intriguing. Since this molecule has a central linear partial chain but no chain ends, it is mysterious that whether it can also spontaneously cause the intermolecular ring-linear penetration or not. To investigate the relationship between the polymer chain architectures including ring structures and their viscoelastic properties is highly significant to understand the polymer chain dynamics from the basis. Until now, there are several reports on the synthesis of these ring-based polymers,[12-14,98-119] however, most of them are unsuitable for the accurate measurements of their various physical properties due to their low molecular weights, broader distribution, uncertain architecture and unguaranteed purity.

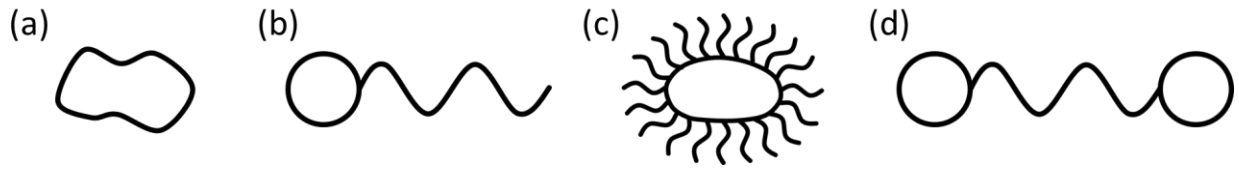

Figure 1-1. Schematic illustrations of ring-based polymers with various architectures: (a) trivial ring, (b) tadpole-shaped, (c) comb-shaped ring and (d) dumbbell-shaped polymers.

In this thesis, first a series of highly-purified ring polymers with wide molecular weight range was aimed to prepare and their viscoelastic properties were investigated to elucidate the ring chain dynamics. Next, three kinds of ring-based polymers, i.e., tadpole-shaped, comb-shaped ring and dumbbell-shaped polymers were proposed to precisely prepare and their viscoelastic properties were extensively investigated to understand the relationships between the chain architectures and their dynamics.

1.4. Outline of this thesis

In Chapter 2 of this thesis, a series of highly-purified trivial rings and three kinds of ring-based polymers, i.e., tadpole-shaped, comb-shaped ring and dumbbell-shaped polymers were precisely prepared by anionic polymerizations, followed by multistep HPLC fractionations. Moreover, all of the samples obtained were characterized accurately.

In Chapter 3, viscoelastic properties of a series of highly-purified trivial ring polymers with wide molecular weight range were investigated and their relaxation mechanisms were discussed.

In Chapter 4, viscoelastic properties of a series of tadpole-shaped polymers with a common ring and linear tails having three different lengths were studied. Their relaxation mechanisms were discussed in terms of the tail chain length dependence.

In Chapter 5, viscoelastic properties of a series of comb-shaped ring polymers with a common ring and linear branches having three different lengths were investigated by comparing with the linear counterparts, while in Chapter 6, viscoelastic properties of a dumbbell-shaped polymer were reported.

Finally in Chapter 7, all of the results obtained in the above chapters were summarized.

1.5. References

1. Roovers, J. (ed.) *Adv. Polym. Sci.; Branched Polymers I*, vol. 142; Springer, Berlin, 1999.
2. Roovers, J. (ed.) *Adv. Polym. Sci.; Branched Polymers II*, vol. 143; Springer, Berlin, 1999.
3. Freifelder, D.; Kleinschmidt, A. K.; Sinsheimer, R. L. *Science* **1964**, *146*, 254-255.
4. Semlyen J. A. (ed.) Cyclic Polymers, 2nd ed.; Kluwer Acad. Publ., Dordrecht, Boston, 2000.
5. Kricheldolf, H. R.; Schwarz, G. *Macromol. Rapid Commun.* **2003**, *24*, 359-381.
6. Dodgson, K.; Semlyen, J. A. *Polymer* **1997**, *18*, 1265-1268.
7. Hild, G.; Kohler, H.; Remmp, P. *Eur. Polym. J.* **1980**, *16*, 525-527.
8. Geiser, D.; Hocker, H. *Macromolecules* **1980**, *13*, 653-656.
9. Roovers, J.; Toporowski, P. M. *Macromolecules* **1983**, *16*, 843-849.
10. Bielawski, C. W.; Benitez, D.; Grubbs, R. H. *Science* **2002**, *297*, 2041-2044.
11. Endo, K. *Adv. Polym. Sci.* **2008**, *217*, 121-183.
12. Kricheldolf, H. R. *J. Polym. Sci.: Part A* **2010**, *48*, 251-284.
13. Yamamoto, T.; Tezuka, Y. *Cyclic and Multicyclic Topological Polymers, in Complex Macromolecular Architectures: Synthesis, Characterization, and Self-Assembly*; John Wiley & Sons (Asia) Pte Ltd, Singapore, 2011.
14. Jia, Z.; Monteiro, M. J. *J. Polym. Sci.: Part A* **2012**, *50*, 2085-2097.
15. Brown, H. A.; Waymouth, R. M. *Acc. Chem. Res.* **2013**, *46*, 2585-2596.
16. Kramer, H. A. *J. Chem. Phys.* **1946**, *14*, 415-424.
17. Zimm, B. H.; Stockmayer, W. H. *J. Chem. Phys.* **1949**, *17*, 1301-1314.
18. Casassa, E. F. *J. Polym. Sci.: Part A* **1965**, *3*, 605-614.
19. Boots, H.; Deutch, J. M. *Macromolecules* **1977**, *10*, 1163-1164.
20. Burchard, W.; Schmidt, M. *Polymer*, **1980**, *21*, 745-749.
21. Prentis, J. J. *J. Chem. Phys.* **1982**, *76*, 1574-1583.
22. Douglas, J. F.; Freed, K. F. *Macromolecules* **1984**, *17*, 2344-2354.
23. Cates, M. E.; Deutsch, J. M. *J. Phys. (Paris)* **1986**, *47*, 2121-2128.
24. Tanaka, F. *J. Chem. Phys.* **1987**, *87*, 4201-4206.
25. Iwata, K. *Macromolecules* **1989**, *22*, 3702-3706.
26. Grosberg, A. Y. *Phys. Rev. Lett.* **2000**, *85*, 3858-3861.
27. Sakaue, T. *Phys. Rev. Lett.* **2011**, *106*, 167802.
28. Wedgewood, L. E.; Ostrov, D. N.; Bird, R. B. *J. Non-Newtonian Fluid Mech.* **1991**, *40*, 119-139.
29. Watanabe, H.; Inoue, T.; Matsumiya, T. *Macromolecules* **2006**, *39*, 5149-5426.
30. Klein, J. *Macromolecules* **1986**, *19*, 105-118.
31. Rubinstein, M. *Phys. Rev. Lett.* **1986**, *57*, 1263-1266.
32. Obukhov, S. P.; Rubinstein, M. *Phys. Rev. Lett.* **1994**, *73*, 1263-1266.
33. Milner, S. T.; Newhall, J. D. *Phys. Rev. Lett.* **2010**, *105*, 208302.

34. Müller, M.; Wittmer, J. P.; Cates, M. E. *Phys. Rev. E* **1996**, *53*, 5063-5074.
35. Brown, S.; Szamel, G. *J. Chem. Phys.* **1998**, *108*, 4705-4708.
36. Brown, S.; Szamel, G. *J. Chem. Phys.* **1998**, *109*, 6184-6192.
37. Müller, M.; Wittmer, J. P.; Cates, M. E. *Phys. Rev. E* **2000**, *61*, 4078-4089.
38. Hur, K.; Winkler, R. G.; Yoon, D. Y. *Macromolecules* **2006**, *39*, 3975-3977.
39. Iyer, B. V.; Lele, A. K.; Shanbhag *Macromolecules* **2007**, *40*, 5995-6000.
40. Subramanian, G.; Shanbhag *Macromolecules* **2008**, *41*, 7239-7242.
41. Suzuki, J.; Takano, A.; Deguchi, T.; Matsushita, Y. *J. Chem. Phys.* **2009**, *131*, 144902.
42. Yang, Y. B.; Sun, Z. Y.; Fu, C. L.; An, L. J.; Wang, Z. G. *J. Chem. Phys.* **2010**, *133*, 064901.
43. Subramanian, G. *J. Chem. Phys.* **2010**, *133*, 164902.
44. Tsolou, G.; Statiks, N.; Baig, G.; Stephanou, P. S.; Mavrantzas, V. G. *Macromolecules* **2010**, *43*, 10692-10713.
45. Hur, K.; Jeong, C.; Winkler, R. G.; Lacevic, N.; Gee, R. H.; Yoon, D. Y. *Macromolecules* **2011**, *44*, 2331-2315.
46. Rosa, A.; Orlandini, E.; Tubiana, L.; Micheletti, C. *Macromolecules* **2011**, *44*, 8668-8680.
47. Halverson, J. D.; Lee, W. B.; Grest, G. S.; Grosberg, A. Y.; Kremer, K. *J. Chem. Phys.* **2011**, *134*, 204904.
48. Halverson, J. D.; Lee, W. B.; Grest, G. S.; Grosberg, A. Y.; Kremer, K. *J. Chem. Phys.* **2011**, *134*, 204905.
49. Halverson, J. D.; Grest, G. S.; Grosberg, A. Y.; Kremer, K.: *Phys. Rev. Lett.* **2012**, *108*, 038301.
50. Reigh, S. Y.; Yoon, D. Y. *ACS Macro Lett.* **2013**, *2*, 296-300.
51. Lo, W. C.; Turner, M. S. *Eur. Polym. J.* **2013**, *102*, 58005.
52. Ida, D. *Polym. J.* **2014**, *46*, 399-404.
53. Smrek, J.; Grosberg, A. Y. *J. Phys.: Condens. Matter* **2015**, *27*, 064117.
54. Lee, E.; Kim, S.; Jung, Y.; *Macromol. Rapid Commun.* **2015**, *36*, 1115-1121.
55. Higgins, J. S.; Dodgson, K.; Semlyen, J. S. *Polymer* **1979**, 20, 553-558.
56. Edwards, C. J. C.; Stepto, R. F. T.; Semlyen, J. A. *Polymer* **1982**, *23*, 869-872.
57. Roovers, J. *J. Polym. Sci.: Polym. Phys. Ed.* **1985**, *23*, 1117-1126.
58. Arrighi, V.; Gagliardi, S.; Dagger, A. C.; Semlyen, J. A.; Higgins, J. S. *Macromolecules* **2004**, *37*, 8057-8065.
59. Ohta, Y.; Kushida, Y.; Matsushita, Y.; Takano, A. *Polymer* **2009**, *50*, 1297-1299.
60. Takano, A.; Kushida, Y.; Ohta, Y.; Masuoka, K.; Matsushita, Y. *Polymer* **2009**, *50*, 1300-1303.
61. Takano, A.; Ohta, Y.; Masuoka, K.; Matsubara, K.; Nakano, T.; Hieno, A.; Itakura, M.; Takahashi, K.; Kinugasa, S.; Kawaguchi, D.; Takahashi, Y.; Matsushita, Y. *Macromolecules* **2012**, *45*, 369-373.
62. Ohta, Y.; Nakamura, M.; Matsushita, Y.; Takano, A. *Polymer* **2012**, *53*, 466-470.
63. Gooβen, S.; Bras, A. R.; Pyckhout-Hintzen, W.; Wischnewski, A.; Richter D.; Rubinstein, M.; Roovers, J.; Lutz, P. J.; Jeong, Y.; Chang, T.; Vlassopoulos, D. *Macromolecules* **2015**, *48*, 1598-1605.
64. Roovers, J. *Macromolecules* **1985**, *18*, 1359-1361.
65. McKenna, G. B.; Hadziioannou, G.; Lutz, P.; Hild, G.; Strazielle, C.; Straupe, C.; Remmp, P.; Kovacs, A.J. *Macromolecules* **1987**, *20*, 498-512.
66. Mills, P. J.; Mayer, J. W.; Kramer, E. J.; Hadziioannou, G.; Lutz, P.; Stazielle, C.; Rempp, P.; Kovacs, A. J. *Macromolecules* **1987**, *20*, 513-518.

67. Roovers, J. *Macromolecules* **1988**, *21*, 1517-1521.
68. Orrah, D. J.; Semlyen, J. A.; Ross-Murphy, S. B. *Polymer* **1988**, *29*, 1452-1454.
69. Orrah, D. J.; Semlyen, J. A.; Ross-Murphy, S. B. *Polymer* **1988**, *29*, 1455-1458.
70. McKenna, G. B.; Hostetter, B. J.; Hadjichristidis, N.; Fetters, L. J.; Plazek, D. J. *Macromolecules* **1989**, *22*, 1834-1852.
71. Tead, S. F.; Kramer, E. J.; Hadziioannou, G.; Antonietti, M.; Sillescu, H.; Lutz, P.; Stazielle, C. *Macromolecules* **1992**, *25*, 3942-3947.
72. Cosgrove, T.; Griffiths, P. C. *Macromolecules* **1992**, *25*, 6761-6764.
73. Griffiths, P. C.; Stilbs, P.; Yu, G. E.; Booth, C. *J. Chem. Phys.* **1995**, *99*, 16752-16756.
74. Santangelo, P. G.; Roland, C. M.; Chang, T.; Cho, D.; Roovers, J. *Macromolecules* **2001**, *34*, 9002-9005.
75. Kawaguchi, D.; Masuoka, K.; Takano, A.; Tanaka, K.; Nagamura, T,; Torikai, N.; Dalgliesh, R. M.; Langridge, S.; Matsushita, Y. *Macromolecules* **2006**, *39*, 5180-5182.
76. Robertson, R. M.; Smith, D. E. *Macromolecules* **2007**, *40*, 3373-3377.
77. Kapnistos, M.; Lang, M.; Vlassopoulos, D.; Pyckhout-Hintzen, W.; Richter, D.; Cho, D.; Chang, T.; Rubinstein, M. *Nat. Mater.* **2008**, *7*, 997-1002.
78. Nam, S.; Leisen, J.; Breedveld, V.; Beckham, H. W. *Polymer* **2008**, *49*, 5467-5473.
79. Nam, S.; Leisen, J.; Breedveld, V.; Beckham, H. W. *Macromolecules* **2009**, *42*, 3121-3128.
80. Bras, A. R.; Pasquino, R.; Koukoulas, T.; Tsolou, G.; Holderer, O.; Radulescu, A.; Allgaier, J.; Mavrantzas, V. G.; Pyckhout-Hintzen, W.; Wischnewski, A.; Vlassopoulos, D.; Richter D. *Soft Matter*, **2011**, *7*, 11169-11176.
81. Kawaguchi, D.; Ohta, Y.; Takano, A.; Matsushita, Y. *Macromolecules* **2012**, *45*, 6748-6752.
82. Pasquino, R.; Vasilakopoulos, T. C.; Jeong, Y. C.; Lee, H.; Rogers, S.; Sakellariou, G.; Allgaier, J.; Takano, A.; Bras, A. R.; Chang, T.; Gooβen, S.; Pyckhout-Hintzen, W.; Wischnewski, A.; Hadjichristidis, N.; Richter, D; Rubinstein, M.; Vlassopoulos, D. *ACS Macro Lett.* **2013**, *2*, 874-878.
83. Bras, A. R.; Gooβen, S.; Krutyeva, M.; Radulescu, A.; Farago, B.; Allgaier, J.; Pyckhout-Hintzen, W.; Wischnewski, A.; Richter D. *Soft Matter*, **2014**, *10*, 3649-3655.
84. Gooβen, S.; Bras, A. R.; Krutyeva, M.; Sharp, M.; Falus, P.; Feoktystov, A.; Gasser, U.; Pyckhout-Hintzen, W.; Wischnewski, A.; Richter D. *Phys. Rev. Lett.* **2014**, *113*, 168302.
85. Gooβen, S.; Krutyeva, M.; Sharp, M.; Falus, P.; Feoktystov, A.; Allgaier, J.; Pyckhout-Hintzen, W.; Wischnewski, A.; Richter D. *Phys. Rev. Lett.* **2015**, *115*, 148302.
86. Rouse, P. E. *J. Chem. Phys.* **1953**, *21*, 1272-1280.
87. de Gennes, P. G. *Scaling Concept in Polymer Physics*; Cornell University: Ithaca, NY, 1979.
88. Doi, M.; Edward, S. F. *The Theory of Polymer Dynamics*; Clarendon: Oxford, UK, 1986.
89. Watanabe, H. *Prog. Polym. Sci.* **1999**, *24*, 1253-1403.
90. McLeish, T. C. B. *Adv. Phys.* **2002**, *51*, 1379-1527.
91. Rubinstein, M.; Colby, R. H. *Polymer Physics*; Oxford University Press: New York, 2003.
92. McLeish, T. B. C. *Europhys. Lett.* **1988**, *6*, 511-516.
93. Pasch, H. Trathnigg, B. *HPLC of Polymers*; Springer: Berlin, 1998.
94. Lee, H. C.; Lee, H.; Lee, W.; Chang, T.; Roovers, J. *Macromolecules* **2000**, *33*, 8119-8121.

95. Kasianowicz, J. J.; kellermayer, M. S. Z.; Deamer, D. W. (eds.) *Structure and Dynamics of Confined Polymers*; Springer: Dordrecht , Netherlands, 2002.
96. Wenz, G.; Han, B. H.; Muller, A. *Chem. Rev.* **2006**, *106*, 782-817.
97. Harada, A.; Takashima, Y.; Yamaguchi, H. *Chem. Soc. Rev.* **2009**, *38*, 875-882.
98. Beinat, S.; Schapparcher, M.; Deffieux, A. *Macromolecules* **1996**, *29*, 6737-6743.
99. Kubo, M.; Hayashi, T.; Kobayashi, H.; Itoh, T. *Macromolecules* **1998**, *31*, 1053-1057.
100. Oike, H.; Washizuka, M.; Tezuka, Y. *Macromol. Rapid Commun.* **2001**, *22*, 1128-1134.
101. Oike, H.; Uchibori, A.; Tsuchitani, A.; Kim, H.K.; Tezuka, Y. *Macromolecules* **2004**, *37*, 7595-7601.
102. Adachi, K.; Irie, H.; Sato, T.; Uchibori, A.; Shiozawa, M.; Tezuka, Y. *Macromolecules* **2005**, *38*, 10210-10219.
103. Li, H.; Debuigne, A.; Jerome, R.; Lecomte, P. *Angew. Chem., Int. Ed.* **2006**, *45*, 2264-2267.
104. Li, H.; Jerome, R.; Lecomte, P. *Polymer* **2006**, *47*, 8406-8413.
105. Li, H.; Riva, R.; Jerome, R.; Lecomte, P. *Macromolecules* **2007**, *40*, 824-831.
106. Shi, G.; Tang, X.; Pan, C. *J. Polym. Sci., Part A* **2008**, *46*, 2390-2401.
107. Dong, Y.; Tong, Y.; Dong, B.; Du, F.; Li, Z. *Macromolecules* **2009**, *42*, 2940-2948.
108. Li, L.; He, W.; Li, J.; Han, S.; Sun, X.; Zhang B. *J. Polym. Sci., Part A* **2009**, *47*, 7066-7077.
109. Wan, X.; Liu, T.; Liu, S. *Biomacromolecules* **2011**, *12*, 1146-1154.
110. Lonsdale, D. E.; Monteiro, M. J. *J. Polym. Sci., Part A* **2011**, *49*, 4603-4612.
111. Dedeoglu, T.; Durmaz, H.; Hizal, G.; Tunca, U. *J. Polym. Sci., Part A* **2012**, *50*, 1917-1925.
112. Wang, G.; Hu, B.; Fan, X.; Zhang, Y.; Huang, J. *J. Polym. Sci., Part A* **2012**, *50*, 2227-2235.
113. Huang, B.; Fan, X.; Wang, G.; Zhang, Y.; Huang, J. *J. Polym. Sci., Part A* **2012**, *50*, 2444-2451.
114. Fan, X.; Huang, B.; Wang, G.; Huang, J. *Polymer* **2012**, *53*, 2890-2896.
115. Schapparcher, M.; Billaud, C.; Paulo, C.; Deffieux, A. *Macromol. Chem. Phys.* **1999**, *200*, 2377-2386.
116. Jia, Z.; Fu, Q.; Huang, J. *Macromolecules* **2006**, *39*, 5190-5193.
117. Li, H.; Jerome, R.; Lecomte, P. *Macromolecules* **2008**, *41*, 650-654.
118. Coulembier, O.; Moins, S.; Winter, J. D.; Gerbaux, P.; Leclere, P.; Lazzaroni, R.; Dubois, P. *Macromolecules* **2010**, *43*, 575-579.
119. Lahasky, S. H.; Serem, W. K.; Guo, L.; Garno, J. C.; Zhang, D. *Macromolecules* **2011**, *44*, 9063-9074.

Chapter 2

Preparation and Characterization of Ring-based Polymers with Various Architectures

Partly adapted with permission from
Doi, Y. et al. *Macromolecules* **2013**, *46*, 1075-1081.[1]

Abstract: Highly-purified trivial ring polymers and also three kinds of ring-based polymers, i.e., (a) tadpole-shaped, (b) dumbbell-shaped and (c) comb-shaped ring polymers, as schematically illustrated in Figure 2-1, were successfully prepared by anionic polymerizations followed by multistep high performance liquid chromatography (HPLC) fractionations. All of the samples obtained were characterized by size exclusion chromatography with multi-angle light scattering (MALS) detector, SEC-MALS measurements and interaction chromatography (IC) measurements. All ring-based polymers were confirmed to have definite architectures with ultrahigh purity over 99%. Therefore, these samples are conceived to be suitable for investigating their physical properties, such as solution and viscoelastic properties accurately in the following chapters.

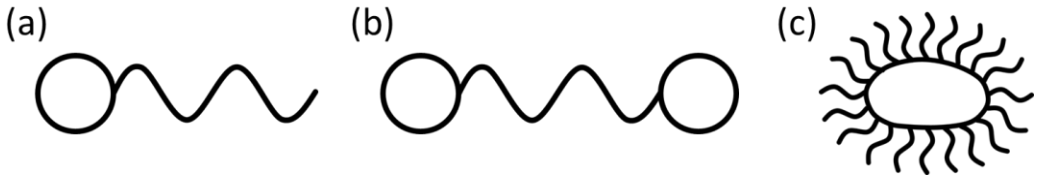

Figure 2-1. Schematic illustrations of ring-based polymers with various architectures: (a) tadpole-shaped, (b) dumbbell-shaped and (c) comb-shaped ring polymers.

2.1. Introduction

Ring polymers are one of the most fascinating model polymers in a view point of polymer physics because they have no chain ends in their structure. This intrinsic feature may give several interesting physical properties. Nevertheless, their accurate physical properties have been mostly unrevealed due to difficulty in preparation of truly pure ring samples. Not only the trivial rings, but also ring-based polymers where ring and linear chains are introduced in one molecule are expected to exhibit intriguing physical properties, which are originated from their unique chain architectures. Several studies on the synthesis of these ring-based polymers have been conducted.[2-4] However, most of them are not suitable for the measurements of their various physical properties with high accuracy due to their low molecular weights, their broader distribution, uncertain architecture or unguaranteed purity. Therefore, there are few cases to investigate their accurate physical properties until now.

In this chapter, highly-purified ring polymers, and three kinds of ring-based polymers, i.e., tadpole-shaped, dumbbell-shaped and comb-shaped ring polymers were prepared by anionic polymerizations followed by separation and purification by multistep high performance liquid chromatography (HPLC). All of the samples obtained were carefully characterized by size exclusion chromatography with a multiangle light scattering detector (SEC-MALS) and interaction chromatography (IC) measurements to confirm their precise architectures.

2.2. Experimental

2.2.1. Preparation of highly-purified ring polystyrenes.

Highly-purified ring polystyrene (PS) samples were prepared in the same manner as reported previously.[5] All operations were carried out in sealed glass apparatuses with breakseals under high-vacuum (~ 1×10^{-3} Pa). In this study, six ring PSs, whose molecular weights covering 10 to 240 kg/mol were prepared. First, telechelic linear PSs with 1,1-diphenylethylene (DPE) type vinyl groups on both ends were anionically synthesized from a styrene monomer with potassium naphthalenide (Naph-K) as an initiator in THF, followed by two-step end-capping reactions with DPE and 1-[3-(3-chloropropyldimethylsilyl)phenyl]-1-phenylethylene (DPE-Cl), as shown in Scheme 2-1. The telechelic PSs were cyclized in dilute THF solution, where excess amount of Naph-K was added to the solution as a coupling agent, as shown in Scheme 2-2. The cyclization products were treated by multistep SEC and IC fractionations to exclude polycondensation products and to isolate ring polymers with high purity over 99.5 % in every case. Before HPLC fractionations, some of the cyclization products were treated by precipitational fractionations in cyclohexane. The sample codes include the initial L and R as linear and ring polymers, and the numerical numbers are followed to express their molecular weights in the unit of kg/mol.

Scheme 2-1. Synthetic scheme of telechelic linear PS with DPE-type double bonds on both ends

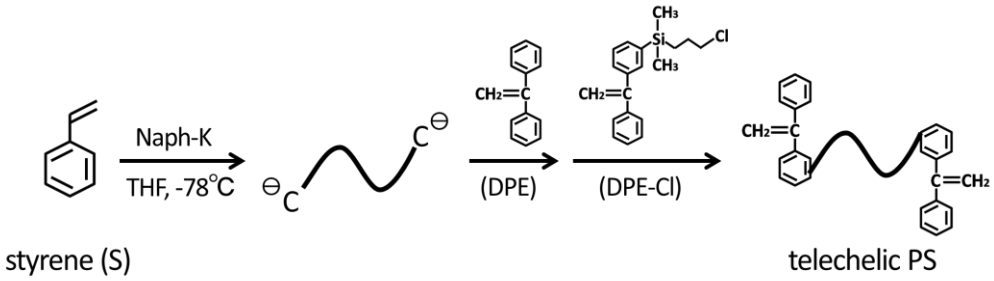

Scheme 2-2. Synthetic scheme of highly-purified ring PS

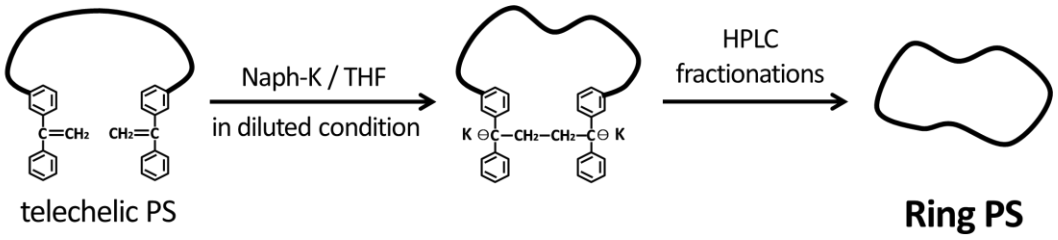

2.2.2. Preparation of tadpole-shaped polystyrenes.

Tadpole-shaped PS samples were anionically synthesized by a coupling reaction between a ring PS and an excess molar amount of living linear PS.[1] Firstly, a highly-purified ring PS, R-60 (M_w = 59.8 kg/mol), with two DPE-type vinyl groups at the coupling point was prepared by the cyclization of a telechelic linear PS, followed by the capping reactions with DPE and DPE-Cl, as shown in Scheme 2-3. The cyclization product was treated by multistep HPLC fractionations. As the next step reactions, three living linear PSs, L-30, L-70 and L-120 (M_w = 27.1, 68.9 and 122 kg/mol, respectively), were anionically synthesized with *sec*-butyllithium (*sec*-BuLi) as an initiator, and each of them was reacted with R-60, as shown in Scheme 2-4. In this synthetic pathway, two kinds of tadpoles which possess one and two linear tail chains in a molecule, single-tail and twin-tail, respectively, were simultaneously produced. They were isolated separately from the coupling products by multistep HPLC fractionations. The sample codes the tadpole molecules thus prepared include the initial S and T for the number of tails, i.e., single-tail and twin-tail, and the following two numerical numbers represent the molecular weights in the unit of kg/mol for ring and linear chain units.

Scheme 2-3. Synthetic scheme of ring PS with two DPE-type vinyl groups

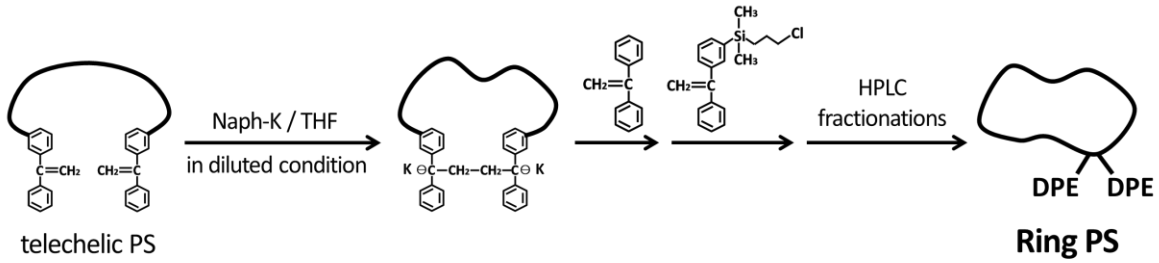

Scheme 2-4. Synthetic scheme of tadpole-shaped PSs

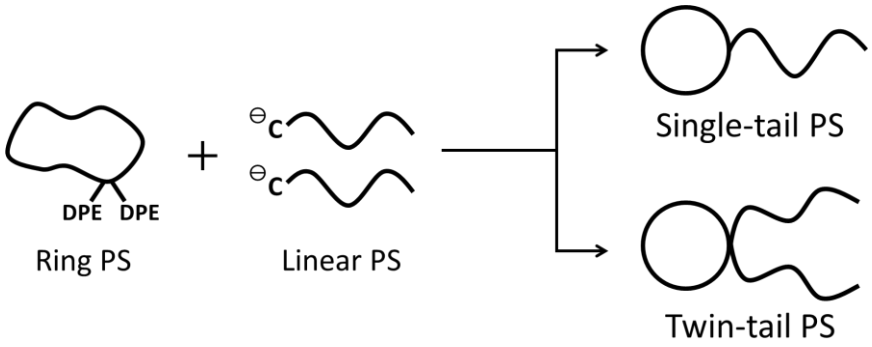

2.2.3. Preparation of dumbbell-shaped polystyrenes.

Dumbbell-shaped PS samples were anionically synthesized by a coupling reaction between an excess molar amount of ring PS and a bifunctional living linear PS. Firstly, a highly-purified ring PS, R-30 (M_w = 33.7 kg/mol), with two DPE-type vinyl groups at the coupling point was prepared in the same manner as shown in Scheme 2-3. Secondly, bifunctional living linear PS was synthesized from Naph-K as an initiator in THF, and reacted with the excess R-30, as shown in Scheme 2-5. In this study, two linear PSs, L-80 and L-240 (M_w are 84.0 and 241 kg/mol, respectively), were used as central linear parts of dumbbell polymers. The coupling products were treated by multistep HPLC fractionations to isolate the dumbbell PS.

Scheme 2-5. Synthetic scheme of dumbbell-shaped polystyrenes

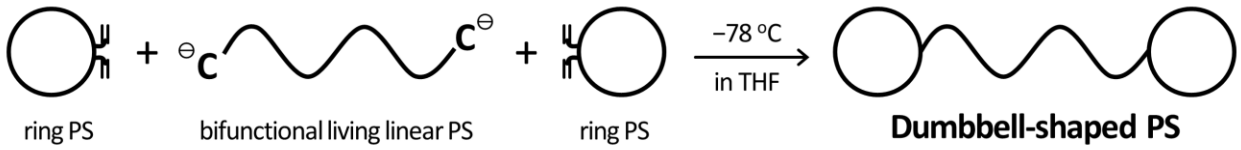

2.2.4. Preparation of comb-shaped ring polystyrenes.

Comb-shaped ring PS samples were anionically synthesized by a chlorosilane coupling reaction between a ring PS backbone and multiple linear PS chains. Scheme 2-6 shows a synthetic route to the ring backbone. Firstly, a telechelic linear polymer with DPE type vinyl groups on both ends was synthesized from a mixed monomer of styrene (S) and 4-(3-butenyl)styrene (BS) (ca. 30/1 mol%) with Naph-K as an initiator in THF. This telechelic polymer was cyclized in dilute THF condition and the product obtained was treated by multistep HPLC fractionations to isolate the ring backbone. To prepare the comb-shaped ring polymers, vinyl groups on BS units in the backbone were functionalized by hydrosilylation reaction with chlorodimethylsilane in benzene and the solution was stirred for one week. This solution was purified by the freeze-drying method. In this study, three linear branches, L-20, L-40 and L-80, were synthesized from *sec*-BuLi as an initiator, and each of them was reacted with the ring backbone. The coupling products were separated by SEC fractionations to isolate the comb-shaped ring samples. Scheme 2-7 shows a synthetic route to the comb-shaped ring PSs. Comb-shaped samples with the linear backbone were also prepared in the same manner but without a cyclization of the backbone, as reference samples. The linear and ring backbones denote LBB and RBB with their molecular weights, while the combs with linear and ring backbones denote LC and RC with a molecular weight of a branch chain in the unit of kg/mol.

Scheme 2-6. Synthetic scheme of the ring backbone

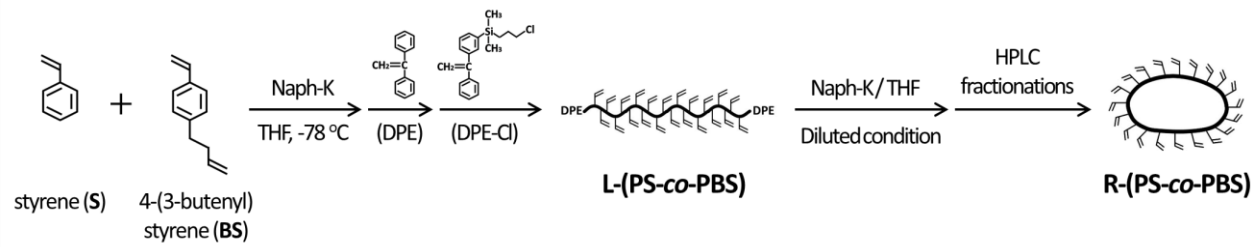

Scheme 2-7. Synthetic scheme of comb-shaped ring PSs

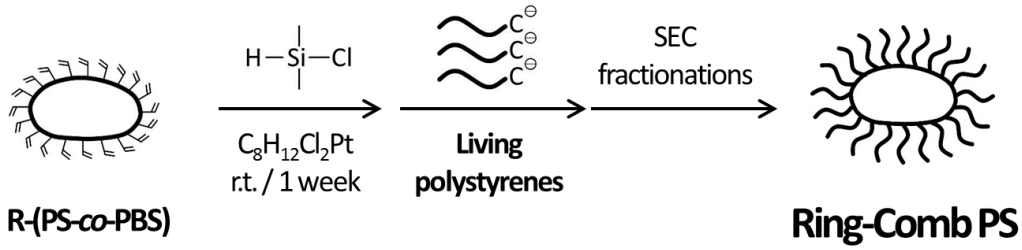

2.2.5. Characterization.

The weight-average molecular weights M_w were determined by multi-angle light scattering (MALS) measurements or size exclusion chromatography (SEC) with MALS detector, i.e., SEC-MALS measurements. MALS measurements were carried out with an apparatus, Dawn EOS (Wyatt Technology Co.), in THF at 35 ^{o}C. SEC-MALS measurements were performed with HPLC system composed of a pump, LC-20AD (Simadzu Co.), a column oven, CTO-20A (Simadzu Co.), a MALS detector, DAWN HELEOS II (Wyatt Technology Co.), and a differential refractive index detector, RID-10A (Simadzu Co.). Two kinds of SEC columns, i.e., silica gel columns (Protein KW-804, Shodex) and polystyrene gel columns (TSK gel G5000H_{HR},

Tosoh Co.), were used according to molecular weights of the samples. The eluent was THF, and the flow rate was 1.0 ml/min. The column temperature was kept constant at 40 ^{o}C. Molecular weight distribution, M_w/M_n, was estimated by SEC measurements with the same HPLC system with a UV detector, SPD-20A (Simadzu Co.), and without the MALS detector. The purity of the trivial ring and ring-based samples was evaluated from IC measurements with the same HPLC system equipped with a handmade column jacket with a thermostatic bath/ circulator, Alpha RA8 (Lauda Co.), instead of the column oven. Two bare-silica gel columns (5SIL10E, Shodex) were used. The eluent was a mixture of *n*-hexane and THF (58/42 in volume) and the flow rate was 3.0 ml/min. The column temperature was adjusted within a range of 10 to 50 ^{o}C to control elution behavior.

2.3. Results and Discussion

2.3.1. Preparation and characterization of highly-purified ring polystyrenes.

Table 2-1 summarizes the molecular characteristics of six telechelic linear PSs used in this study. As an example, a procedure of cyclization and coarse purification process for telechelic L-60 is shown in Figure 2-2. Figure 2-2(a) and (b) show SEC chromatograms of L-60 and its cyclization product, respectively. From the peak area ratio in Figure 2-2(b), this reaction product includes ca. 40% of a ring PS eluted at around 19 min, accompanied by several polycondensation products together with linear molecules as a precursor eluted at 18 min. Figure 2-2(c) shows the chromatogram of the product after the precipitational fractionation. Most of the high molecular weight byproducts were removed and it was found that the fractionated product includes ca. 70% of a ring PS.

Table 2-1. Molecular characteristics of six telechelic linear PSs

Samples	$10^{-3}M_w$ [a]	M_w/M_n [b]
L-10	12.8	1.05
L-20	19.6	1.05
L-40	44.2	1.02
L-60	61.2	1.04
L-90	95.9	1.02
L-240	253	1.03

Estimated from [a]MALS or SEC-MALS, [b]SEC measurements

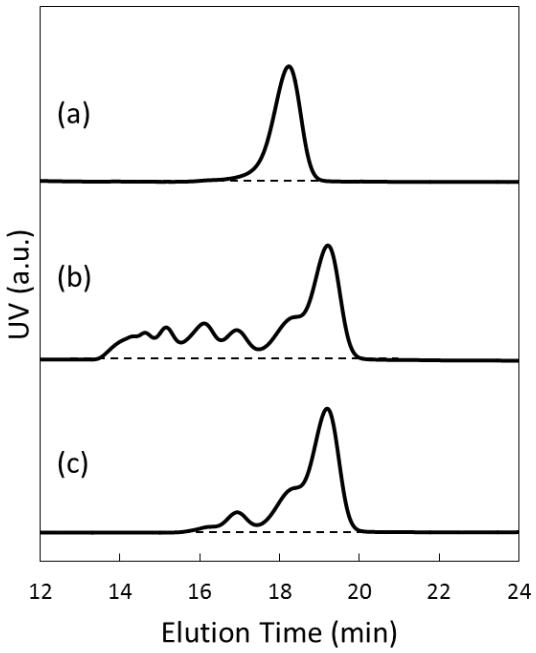

Figure 2-2. SEC chromatograms of (a) L-60, (b) the cyclization product of L-60 and (c) the product after precipitational fractionation. Reprinted with permission from ref. 1.

To exclude the unreacted linear precursor from the fractionated product, successive IC and SEC fractionations were performed for the product after the precipitational fractionation, results being shown in Figure 2-3. After the fractionations, it is evident from Figure 2-3(c) and (f) that ring chains, R-60, were successfully isolated in both IC and SEC modes. The purity of this ring sample can be estimated to be 99.9% from Figure 2-3(c). Using the same procedures, six ring PSs with high purity over 99.5 % were successfully prepared and their characteristics are summarized in Table 2-2. Since all cyclization reactions of telechelic PSs in this study were performed in a good solvent, THF, the fraction of knotted ring products must be negligibly small in the cyclization product, even for the largest ring, R-240, by referring to the previous report.[6]

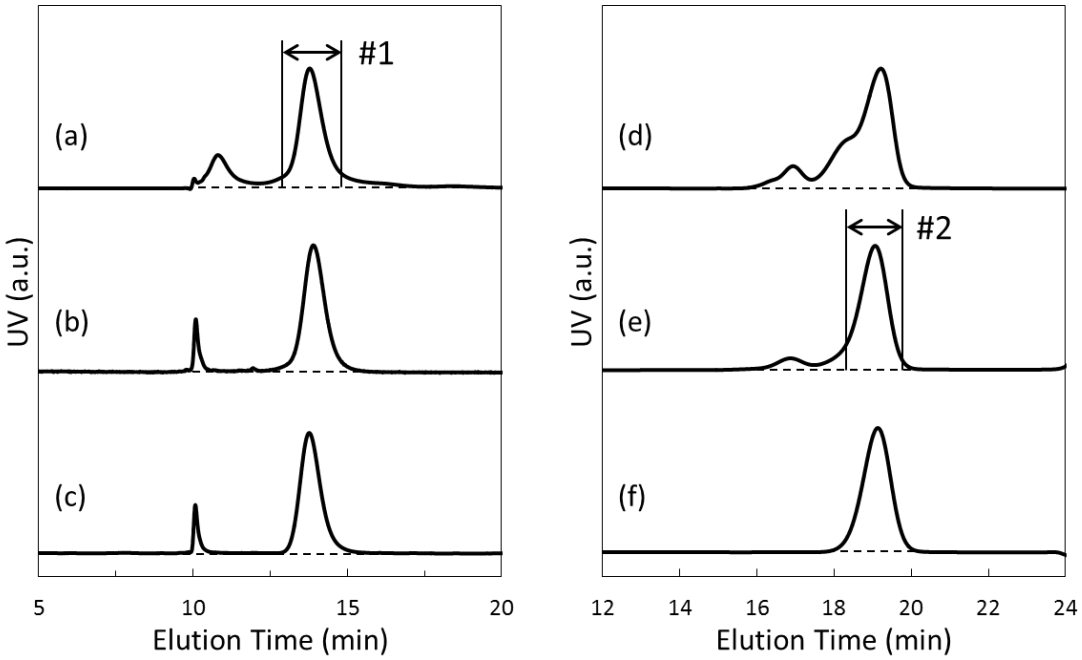

Figure 2-3. IC chromatograms of (a) the cyclization product after precipitational fractionation, (b) the fraction #1 after IC fractionation and (c) the fraction #2 after the IC and SEC fractionations. SEC chromatograms of (d), (e) and (f) are corresponding to the samples (a), (b) and (c), respectively. Reprinted with permission from ref. 1.

Table 2-2. Molecular characteristics of a series of highly-purified ring PSs

Samples	$10^{-3}M_w$ [a]	M_w/M_n [b]	Purity (%) [c]
R-10	12.3	1.05	99.6
R-20	18.4	1.05	99.6
R-40	41.7	1.02	99.7
R-60	59.8	1.02	99.9
R-90	93.0	1.02	99.5
R-240	244	1.02	99.6

Estimated from [a]MALS or SEC-MALS, [b]SEC and [c]IC measurements

2.3.2. Preparation and characterization of tadpole-shaped polystyrenes.

Figure 2-4(a) and (b) show SEC chromatograms for R-60 (M_w = 59.8 kg/mol, M_w/M_n = 1.02, purity = 99.9%) and L-70 (M_w = 68.9 kg/mol, M_w/M_n = 1.02), respectively. After the coupling reaction between them, the product shows the multipeaks in Figure 2-4(c). In this chromatogram, the peak for R-60 mostly disappeared, and two new peaks appeared at two short elution times (15.0 and 16.2 min). This fact suggests that two kinds of tadpoles, i.e., the single-tail, S-60/70, and the twin-tail, T-60/70, were produced simultaneously. These two peaks were isolated separately by multistep HPLC fractionations, as shown in Figure 2-4(d) and (e). The measured absolute weight-average molecular weight of the sample in Figure 2-4(d) is 130 kg/mol, which is in good agreement with the sum of M_w of R-60 and L-70, 129 kg/mol. Likewise, M_w of the sample in Figure 2-4(e), 192 kg/mol, agrees well with the sum of M_w of R-60 and double of M_w for L-70, 198 kg/mol. These results suggest that two tadpole samples were successfully prepared as designed. Figure 2-5 shows IC chromatograms for the two tadpoles, S-60/70 and T-60/70, compared with those for their ring and linear components. In this figure, the peaks for the tadpoles are almost completely separated from that for L-70, and the purities of two tadpoles are estimated to be 99.6% for both.

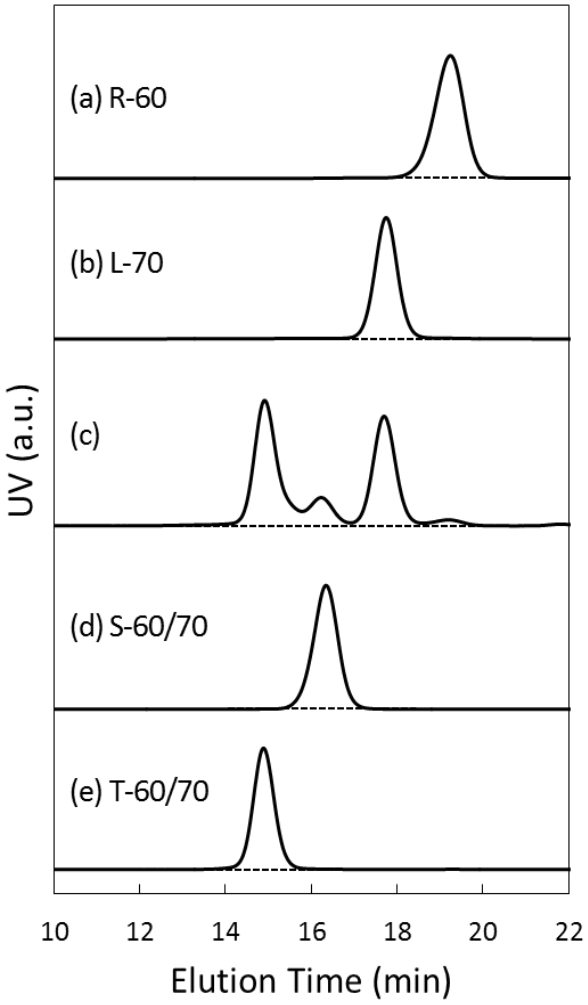

Figure 2-4. SEC chromatograms of (a) R-60, (b) L-70, (c) the coupling product, (d) the isolated S-60/70 and (e) the isolated T-60/70.

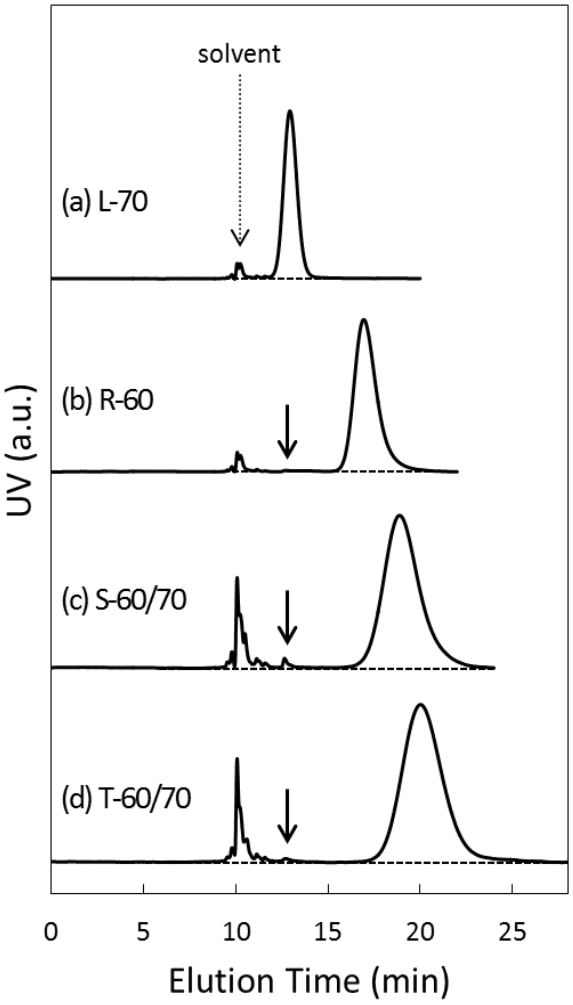

Figure 2-5. IC chromatograms of (a) L-70, (b) R-60, (c) S-60/70 and (d) T-60/70. Reprinted with permission from ref. 7.

Applying the same procedures to the products, a series of highly-purified tadpole samples having a common ring and three different lengths of linear tails were prepared. All samples were confirmed to possess high purities over 99% by IC measurements. Their molecular characteristics are summarized in Table 2-3.

Table 2-3. Molecular characteristics of a series of tadpole-shaped PSs

Samples	$10^{-3}M_w$ [a]	M_w/M_n [b]	$10^{-3}M_{w,tail}$ [a]	$M_w/M_{n,tail}$ [b]	Purity [c]
R-60	59.8	1.02	-	-	99.9
S-60/30	86.8	1.02	27.1	1.02	99.3
T-60/30	114	1.02			99.5
S-60/70	130	1.01	68.9	1.02	99.6
T-60/70	192	1.01			99.6
S-60/120	183	1.02	122	1.03	99.1
T-60/120	300	1.02			99.7

Estimated from [a]SEC-MALS, [b]SEC and [c]IC measurements

2.3.3. Preparation and characterization of dumbbell-shaped polystyrenes.

Figure 2-6(a) and (b) show SEC chromatograms for R-30 (M_w = 33.7 kg/mol, M_w/M_n = 1.02, purity = 99.9 %) and L-80 (M_w = 84.0 kg/mol, M_w/M_n = 1.06), respectively. The dotted curve in Figure 2-6(c) shows the chromatogram after a coupling reaction. In addition to the peak originated from the excess amount of unreacted R-30, a multipeak newly appears at a short elution time (13-18 min). Since this multipeak is considered to be a coupling product, including a dumbbell polymer, multistep HPLC fractionations were performed. Firstly, the excess R-30 was excluded by SEC fractionation, and the chromatogram after the fractionation is shown as the solid curve in Figure 2-6(c). Apparently, this multipeak is mainly composed of three peaks, which are corresponding to the dumbbell molecule as designed, single-tail tadpole and linear polymers, in the order of the shorter elution time.

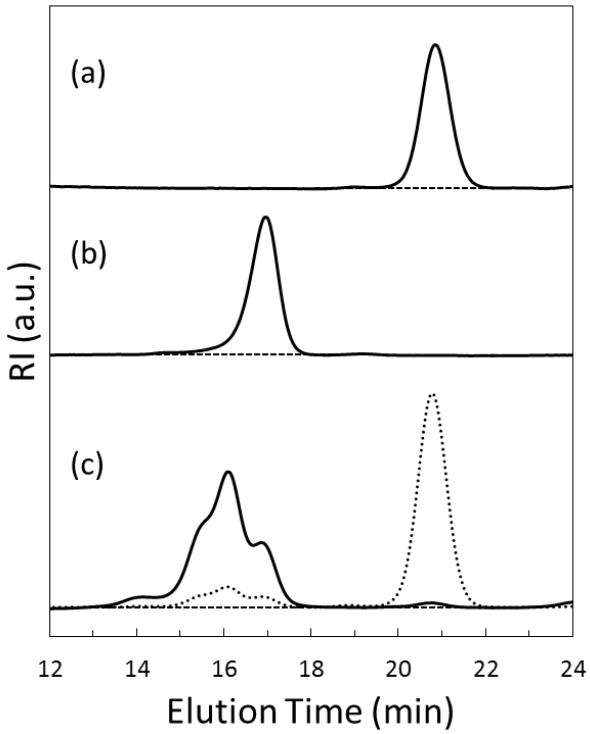

Figure 2-6. SEC chromatograms of D-30/80/30 through a coupling reaction: (a) R-30, (b) L-80 and (c) a coupling product (dotted) and a product after excluding unreacted R-30 (solid).

Secondly, IC measurement for the product after excluding R-30 was performed. The result is shown in Figure 2-7(a). Evidently, three peaks were separated well in IC mode and they are considered to be associated with the linear, single-tail and dumbbell polymers, in the order from the shorter elution time. The sample was fractionated under the condition, and the IC chromatogram of the dumbbell sample obtained is shown in Figure 2-7(b), while the corresponding SEC chromatogram is shown in Figure 2-6(d). It was confirmed that the product shown in Figure 2-7(b) and (d) has a molecular weight of 147 kg/mol, this value is close to the sum, 151 kg/mol, of that of L-80, 84.0 kg/mol, and double of M_w for R-30, 2 × 33.7 = 67.4 kg/mol. This result suggests that the dumbbell polymer was successfully prepared as designed.

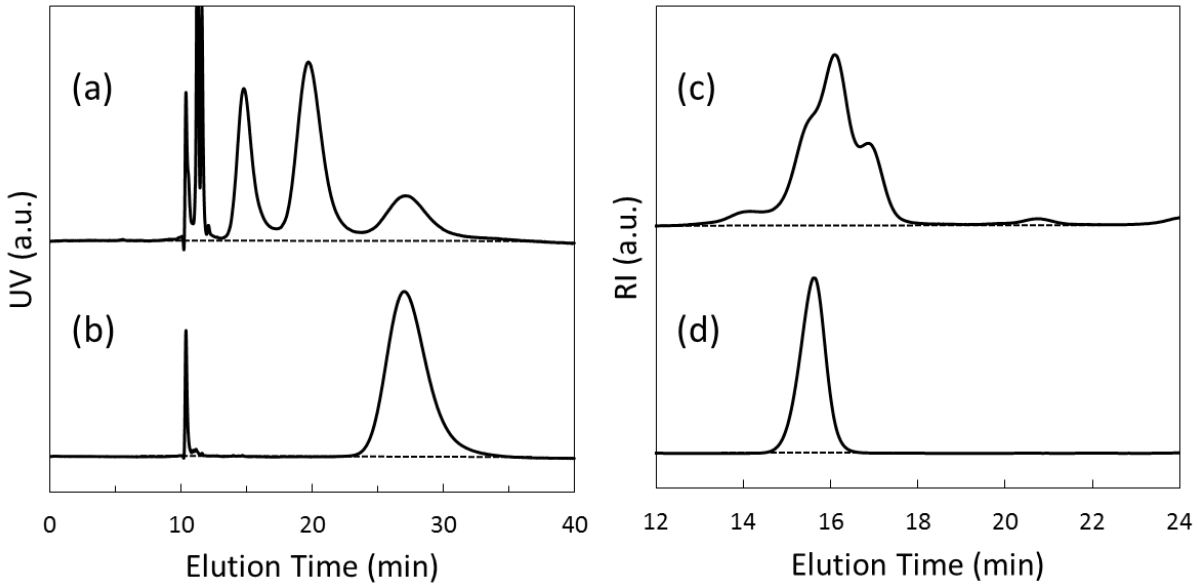

Figure 2-7. IC chromatograms of (a) a coupling product after excluding R-30, (b) the isolated D-30/80/30. SEC chromatograms of (c) and (d) are corresponding to the samples (a) and (b).

Applying the same procedure, a dumbbell PS, D-30/240/30, with a long middle linear chain ($M_{w,linear}$ = 241 kg/mol) was also prepared. Molecular characteristics of two dumbbell samples are summarized in Table 2-4. Both samples were confirmed to possess well-defied dumbbell-shaped structures by SEC-MALS measurements and also to have high purities over 99% by IC measurements.

Table 2-4. Molecular characteristics of dumbbell-shaped polystyrenes

Samples	$10^{-3}M_w$ [a]	$10^{-3}M_{w,ring}$ [a]	$10^{-3}M_{w,linear}$ [a]	M_w/M_n [b]	Purity [c]
D-30/80/30	147	33.7	84.0	1.01	~ 99%
D-30/240/30	301		241	1.01	~ 99%

Estimated by (a) SEC-MALS, (b) SEC and (c) IC measurements

2.3.4. Preparation and characterization of comb-shaped ring polystyrenes.

A telechelic linear poly(styrene-*co*-4-(3-butenyl)styrene) (LBB-70; M_w = 70.9 kg/mol, M_w/M_n = 1.01) was anionically synthesized. A ring backbone, RBB-70, was prepared by the cyclization reaction of LBB-70 followed by multistep HPLC fractionations. Figure 2-8 shows SEC chromatograms for linear (left) and ring (right) backbones with their absolute weight-average molecular weights M_w displayed by a blue and a red line, respectively. The peak for the ring backbone with narrow distribution eluted slower than that for the linear one, while their molecular weights are almost the same. From IC measurements, the ring backbone was confirmed to have high purity over 99%. From ^{1}H-NMR measurements, the number of functional vinyl groups of BS or DPE units, N_f, in the linear and ring backbones was estimated to be 22 and 20, respectively. The results are perfectly consistent with the molecular design, namely the linear precursor has two additional double bonds on two chain ends. Molecular characteristics of the linear and ring backbones are summarized in Table 2-5. From the above, a pair of linear and ring backbones with the same molecular weights and the similar number of BS units was obtained.

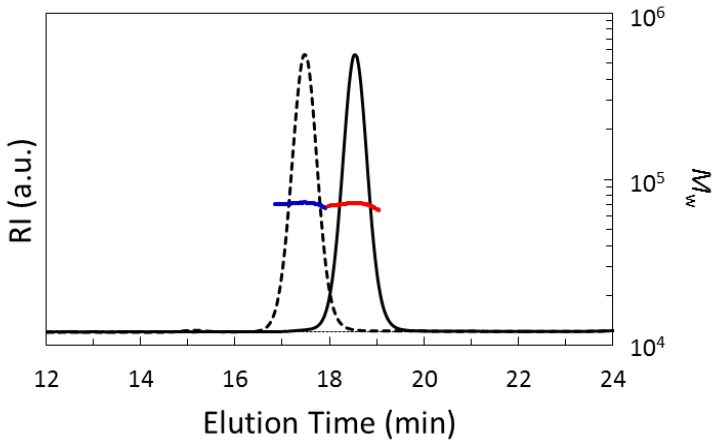

Figure 2-8. SEC chromatograms of LBB-70 (left) and RBB-70 (right) with M_w.

Table 2-5. Molecular characteristics of linear and ring backbones

Samples	$10^{-3}M_w$ [a]	M_w/M_n [b]	N_f [c]	Purity [d]
LBB-70	70.9	1.01	22	-
RBB-70	70.5	1.01	20	~ 99 %

Estimated from [a]SEC-MALS, [b]SEC, [c1]H-NMR and [d]IC measurements

Figure 2-9(a) and (b) compare SEC chromatograms of RBB-70 and L-20, respectively, while Figure 2-9(c) shows the chromatogram after a coupling reaction between them. In this figure, a new unimodal peak has appeared at a shorter elution time (13-15 min), which is considered to be a comb-shaped ring sample, RC-20. This peak was isolated by SEC fractionation, as shown in Figure 2-9(d). In the same manner, three comb-shaped rings as well as the corresponding linear counterparts were prepared. Their molecular characteristics were summarized in Table 2-6. All comb samples were confirmed to be over 99% from SEC measurements. Moreover, all comb samples, except for RC-80, were obtained as designed, while only RC-80 has less number of branches.

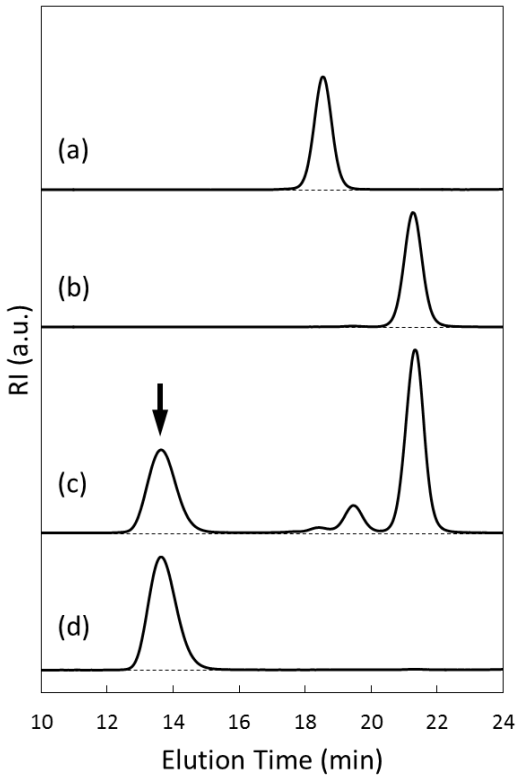

Figure 2-9. SEC chromatograms of RC-20 thorough a coupling reaction: (a) RBB-70, (b) L-20, (c) a coupling product and (d) the isolated RC-20.

Table 2-6. Molecular characteristics of a series of LC and RC samples

Samples	$10^{-3}M_w$ [a]	M_w/M_n [b]	$10^{-3}M_{w,br}$ [a]	f [c]
LC-20	491	1.02	20.2	21
RC-20	434	1.03	19.2	19
LC-40	1070	1.05	41.5	24
RC-40	929	1.04	41.5	21
LC-80	1630	1.07	75.9	21
RC-80	1100	1.14	75.9	14

Estimated from [a]SEC-MALS and [b]SEC measurements. [c]f: the number of branches calculated from $f = (M_w - M_{w,bb})/M_{w,br}$.

2.4. Conclusions

In this chapter, highly-purified trivial ring polymers and also three kinds of ring-based polymers, i.e., tadpole-shaped, dumbbell-shaped and comb-shaped ring polymers were successfully prepared by anionic polymerizations followed by multistep HPLC fractionations. All of the samples obtained were characterized by SEC-MALS and IC measurements, and they were confirmed to have definite architectures with ultrahigh purity over 99%. Therefore, they are conceived to be suitable samples for accurate investigation of their physical properties, such as solution and viscoelastic properties in the following chapters.

2.5. References

1. Doi, Y.; Ohta, Y.; Nakamura, M.; Takano, A.; Takahashi, Y.; Matsushita, Y. *Macromolecules* **2013**, *46*, 1075-1081.
2. Kricheldolf, H. R. *J. Polym. Sci.: Part A* **2010**, *48*, 251-284.
3. Yamamoto, T.; Tezuka, Y. *Cyclic and Multicyclic Topological Polymers, in Complex Macromolecular Architectures: Synthesis, Characterization, and Self-Assembly*; John Wiley & Sons (Asia) Pte Ltd, Singapore, 2011.
4. Jia, Z.; Monteiro, M. J. *J. Polym. Sci.: Part A* **2012**, *50*, 2085-2097.
5. Cho, D.; Masuoka, K.; Koguchi, K.; Asari, T.; Kawaguchi, D.; Takano, A.; Matsushita, Y. *Polym. J.* **2005**, *37*, 506-511.
6. Ohta, Y.; Nakamura, M.; Matsushita, Y.; Takano, A. *Polymer* **2012**, *53*, 466-470.
7. Doi, Y.; Takano, A.; Takahashi, Y.; Matsushita, Y. *Macromolecules* **2015**, *48*, 8667-8674.

Chapter 3

Viscoelastic Properties of Ring Polystyrenes with Ultrahigh Purity

Adapted with permission from

Doi, Y. et al. *Macromolecules* **2015**, *48*, 3140-3147.[1]

Abstract: Viscoelastic properties of highly-purified ring polystyrene (PS) samples with wide molecular weight range were investigated. It has been revealed that all rings in this study exhibit no rubbery plateau and faster terminal relaxation than the linear counterparts. This fact suggests that the relaxation mechanisms for ring polymers are completely different from linear counterparts. The dynamic moduli for rings experimentally obtained were compared with the Rouse ring model. Rings with moderate molecular weights, $2M_e \leq M_w \leq 5M_e$, are apparently in good agreement with the predictions. In contrast, small rings with M_w of $M_w \leq M_e$ and large rings with M_w of $5M_e \leq M_w$ exhibit discrepancy between experimental and calculated data. Moreover, it turned out that two rheological parameters, i.e., zero-shear viscosities, η_0, and steady-state recoverable compliance, J_e, for rings strongly depend on their molecular weights. The small rings apparently give the Rouse like behavior, while rings with moderate M_w ($2M_e \leq M_w \leq 5M_e$) show η_0 supported by the Rouse ring prediction, but reveal J_e of inconsistency with the model. To the contrary, the largest ring with M_w of $5M_e < M_w$ exhibits clearly larger η_0 and J_e than the predicted values by the model, suggesting that some intermolecular interactions are generated.

3.1. Introduction

Ring polymers are one of the most fascinating model polymers, especially from the aspect of the molecular chain dynamics, because they have no chain ends. However, until recently their dynamic properties have not been mostly clarified due to the difficulty in preparation of truly pure ring samples. Therefore, understanding the dynamics of rings is one of the unsolved problems in polymer science for a long period of time.[2] Recently, Kapnistos et al.[3] reported that the pure rings, treated by liquid chromatography at the critical condition (LCCC), show remarkable rheological features: the rings do not exhibit a definite rubbery plateau but power-law decay of the stress relaxation. These results suggest that the ring chains adopt completely different relaxation mechanisms from linear counterparts. However, they used only two ring samples in the report, and hence there still remains an open problem.

In this chapter, the melt viscoelastic properties of a series of highly-purified ring polystyrene (PS) samples with a wide molecular weight range (10-240 kg/mol) were investigated. To elucidate their relaxation mechanisms, their dynamic moduli were directly compared with the Rouse ring model.[4-7] Moreover, the molecular weight dependence of the zero-shear viscosities, η_0, and the steady-state recoverable compliances, J_e, was discussed.

3.2. Experimental

Molecular characteristics of six ring PSs are summarized in Table 3-1.

Viscoelastic properties of ring polymers were investigated by using the ARES-G2 rheometer (TA Instruments) with 8 mm diameter and 0.1 rad angle cone plates, or 8 mm diameter parallel plates. Temperatures for measurements were varied in the range of 120-240 ^{o}C, where the highest temperature was depending on the samples, under the nitrogen atmosphere to prevent chain degradations. The frequency range adopted was 0.1-100 s^{-1} in a linear strain region (< 10 %). Rheological measurements were carried out basically in the same condition from chapter 3 to 6. After the rheological measurements, all samples were tested by SEC and IC to check chain degradations.

Table 3-1. Molecular characteristics of a series of highly-purified ring PSs

Samples	$10^{-3}M_w$ [a]	M_w/M_n [b]	Purity (%) [c]
R-10	12.3	1.05	99.6
R-20	18.4	1.05	99.6
R-40	41.7	1.02	99.7
R-60	59.8	1.02	99.9
R-90	93.0	1.02	99.5
R-240	244	1.02	99.6

Estimated from [a]MALS or SEC-MALS, [b]SEC and [c]IC measurements

3.3. Rheological data analyses

Master curves of the dynamic storage and loss moduli, $G'(\omega)$ and $G''(\omega)$, were constructed by applying the time-temperature superposition (TTS) principle[8] with the reference temperature T_{ref} of 160 ^{o}C. First the data obtained at each temperature were vertically shifted by $b_T = \rho(T_{ref})T_{ref} / \rho(T)T$, where $\rho(T)$ is the density for PS at temperature T, which estimated by the relationship: $\rho(T) = 1.2503 - 6.05 \times 10^{-4}T$.[9] Subsequently, the data were horizontally shifted by a_T, which is so-called temperature dependent shift factor, to attain the best fittings. For linear PSs, the following relationship of a_T was obtained: $\log a_T = -c_1(T - T_{ref})/(c_2 + T - T_{ref})$ with T_{ref} = 160 ^{o}C = 433.15 K, c_1 = 6.3 and c_2 = 112 K.[8]

3.4. Results and Discussion

Figure 3-1 shows the master curves of the storage and loss moduli, $G'(\omega)$ and $G''(\omega)$, for six ring PSs, (a) R-10, (b) R-20, (c) R-40, (d) R-60, (e) R-90 and (f) R-240, compared with their linear counterparts. Figure 3-2 shows the temperature T dependence of the horizontal shift factors a_T for (s) linear and (b) ring PSs. First of all, in Figure 3-1 and 3-2, the time-temperature superposition can hold for all ring samples in this study. After the rheological measurements, all ring samples were confirmed to show little chain degradations by SEC and IC measurements.

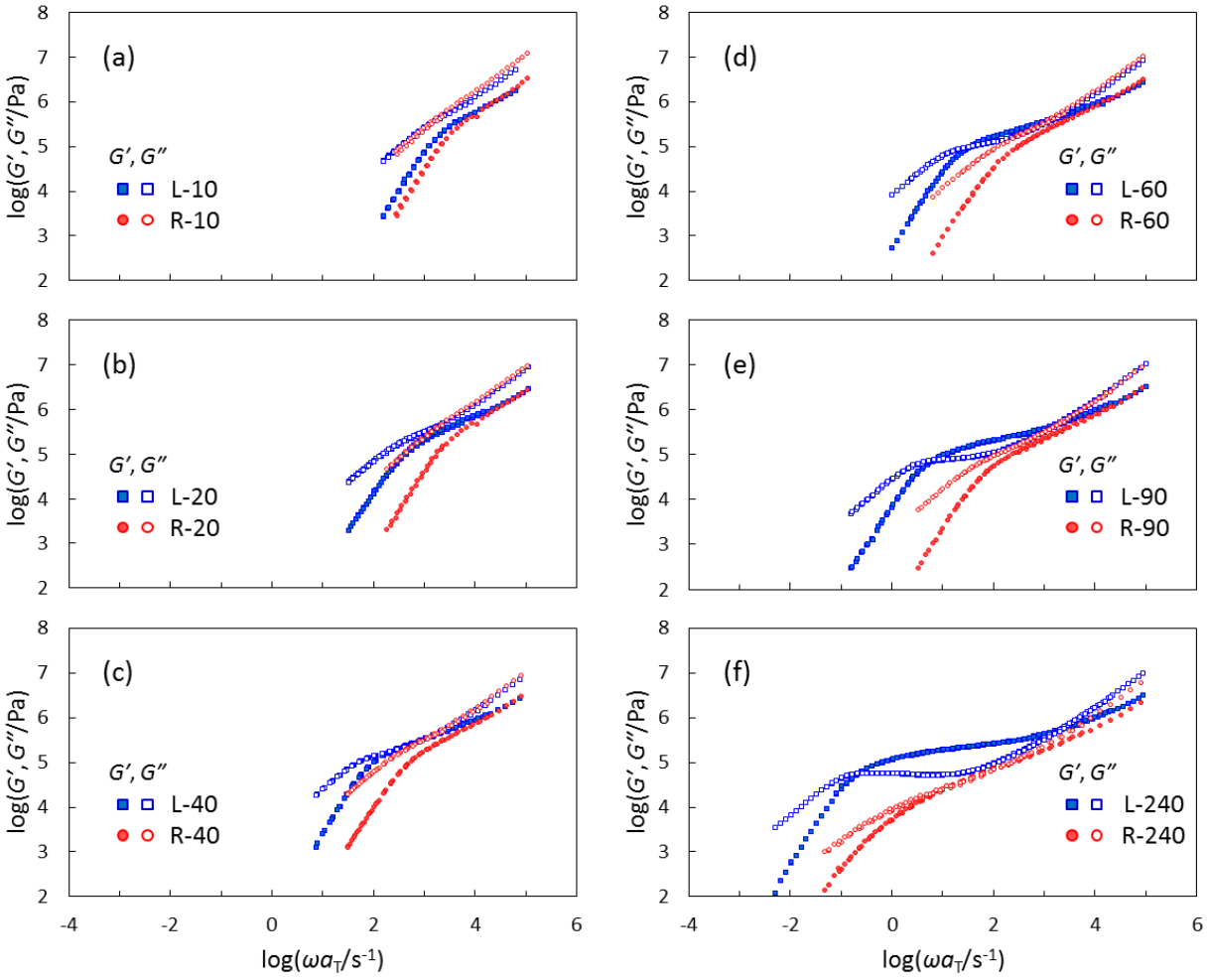

Figure 3-1. Master curves of G' (closed) and G'' (open) for ring PSs compared with those for the linear counterparts at T_{ref} = 160 °C: (a) R-10, (b) R-20, (c) R-40, (d) R-60, (e) R-90 and (f) R-240. Reprinted with permission from ref. 1.

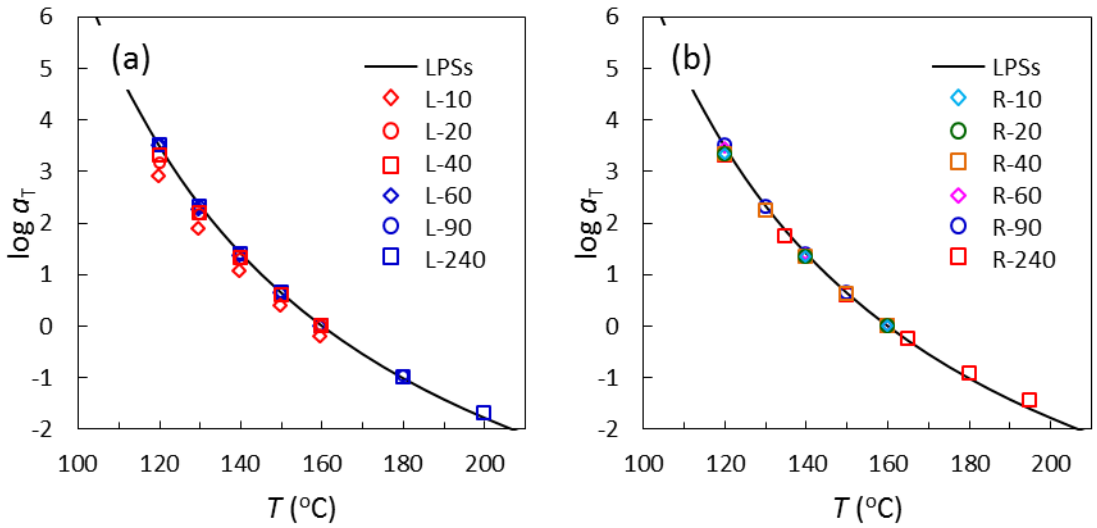

Figure 3-2. Temperature dependence of the horizontal shift factors a_T for (a) linear and (b) ring PSs at T_{ref} = 160 °C. Solid curves indicate the T dependence of a_T for long linear PSs (M_w > 40 kg/mol). Reprinted with permission from ref. 1.

In Figure 3-1, each ring PS shows clearly faster terminal relaxation than its linear counterpart within entire molecular weight range examined in this study. Moreover, linear PSs exhibit a clear rubbery plateau where their molecular weights are larger than the critical entanglement molecular weight M_c (= 36.0 kg/mol), while rings reveal no rubbery plateau even though their molecular weights are sufficiently larger than M_c for linear PSs. These results strongly suggest that the ring chains form little intermolecular entanglements and that they reveal completely different chain relaxation mechanisms from linear ones.

In Figure 3-2 (a), linear PSs with higher molecular weight than 40 kg/mol exhibited common T dependence as represented by the solid curve; $\log a_T = -c_1(T - T_{ref})/(c_2 + T - T_{ref})$ with T_{ref} = 433.15 K, c_1 = 6.3 and c_2 = 112 K.[8] For linear PSs with lower molecular weight than 40 kg/mol, a correction was needed because of their low glass transition temperatures T_g depending on their

molecular weights. In contrast, T dependence of a_T for ring PSs is apparently independent of their molecular weights and is similar to that for long linear PSs, as shown in Figure 3-2 (b). This result implies that a_T for all ring PSs in this study are not necessary to correct, and in other words, T_g for the ring PSs are practically the same as those for long linear PSs, although accurate T_g values for rings in this study were not able to be obtained due to the limitation of the amount of the samples. Previous works also support the hypothesis that T_g for rings are constant without depending on the molecular weights.[10,11]

To examine the relaxation mechanisms of ring polymers, the experimental dynamic moduli were compared with the model prediction. Since all rings in this study are considered to be less-entangled system, the Rouse ring prediction was performed.[4-7] The predicted curves can be expressed by the following equations:

$$G'(\omega) = \frac{2\rho RT}{M_w} \sum_{p\geq 1} \frac{\omega^2 \tau_p^2}{1+\omega^2 \tau_p^2} \tag{3-1}$$

$$G''(\omega) = \frac{2\rho RT}{M_w} \sum_{p\geq 1} \frac{\omega \tau_p}{1+\omega^2 \tau_p^2} + 10^{1.85}\omega \tag{3-2}$$

$$\tau_p = \frac{\tau_{ring}}{p^2}, \qquad \tau_{ring}(M_w) = \frac{\tau_{linear}(M_w)}{4} \quad (\propto M_w{}^2) \tag{3-3}$$

where ρ is the density of polystyrene (= 1.05 g/cm^3), R is the gas constant (= 8.314 JK^{-1}mol^{-1}), T is the temperature at Kelvin unit, p is the mode number and τ_p is the pth Rouse relaxation time. In addition to the Rouse ring functions, the contribution from glassy mode is considered in G'' ($G''_{glass} = 10^{1.85}\omega$) in eq (3-2) to discuss their dynamic behavior in a wide frequency range. In fact, the data up to $\omega = 10^4$ s^{-1} was treated in this study. The longest Rouse relaxation time for a ring

chain, τ_{ring}, is defined as a quarter of that for a Rouse linear chain, τ_{linear}, with the same molecular weight. The second-moment average relaxation time $<\tau>_w$ for the Rouse linear chains is estimated to be $6.18 \times M_w^{2.0}$ in ref. 1, and therefore $<\tau>_w$ for the ideal Rouse ring chains can be calculated. The results of the Rouse ring prediction comparing with the experimental data are shown in Figure 3-3.

In this figure, the experimental data for R-40 agree well with the calculated curves. This result suggests that ring molecules around this molecular weight range apparently behave as Rouse ring chains, which must basically follow the Gaussian chain distribution, although there is no guarantee that the rings in this study have the Gaussian chain conformation. In contrast to R-40, other ring samples reveal a clear deviation from the predicted curves in the terminal region. The experimental data, especially G', for R-90 reveal slightly slower terminal relaxation than the curves calculated. Moreover, R-240 exhibits excessive relaxation delay compared with the prediction. In fact, the experimental $<\tau>_w$ for R-240 is more than 30 times as large as that for the predicted Rouse ring. These results indicate that R-90 exhibits some small intermolecular interactions and that R-240 adopts well-entangled state, although their relaxation mechanisms must be totally different from those for the well-entangled linear chains. To the contrary, the small ring, R-20, exhibits apparently faster terminal relaxation compared with the Rouse ring prediction in Figure 3-3. This difference might be originated from the non-Gaussianity of the small rings' conformation, which induces a change of the viscoelastic segment size. In fact, there is no necessity for ring polymers to follow the Gaussian chain conformation in a whole range of the molecular weights due to the absence of the chain ends. To confirm the ring chain conformation in bulk, further investigations such as small-angle neutron scattering (SANS) measurements are necessary.

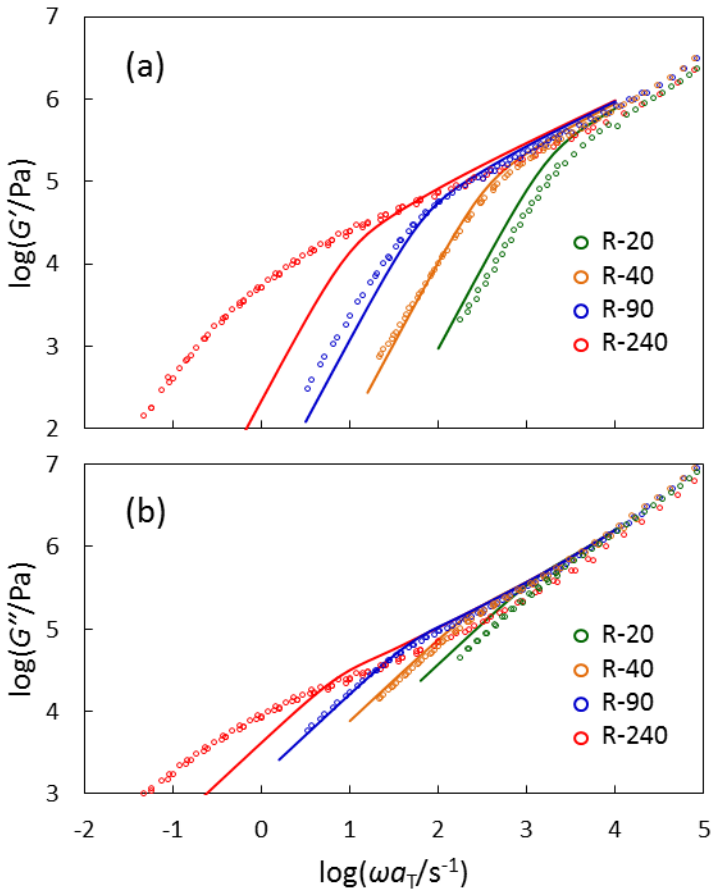

Figure 3-3. Rouse ring model prediction curves (solid lines) of (a) G' and (b) G'' for R-20, R-40, R-90 and R-240, compared with the experimental data (open circles) at T_{ref} = 160 ^{o}C. Reprinted with permission from ref. 1.

From the master curves in Figure 3-1, two rheological parameters, i.e., the zero-shear viscosities, η_0, and the steady-state recoverable compliances, J_e, for all ring samples at T_{ref} = 160 ^{o}C were estimated. Both parameters reflect the characteristic relaxation behavior in the terminal region, represented by the following equations:

$$\eta_0 = \lim_{\omega \to 0} G''(\omega)/\omega \tag{3-4}$$

$$J_e = (1/\eta_0^2) \lim_{\omega \to 0} (G'(\omega)/\omega^2) \tag{3-5}$$

The rheologically important two parameters estimated in a manner as described in ref. 3 and the values obtained were summarized in Table 3-2.

Table 3-2. Rheological parameters, η_0 and J_e, for ring PSs at T_{ref} = 160 ^oC

Samples	$\eta_0 \times 10^{-3}$ (Pa·s)	$J_e \times 10^5$ (Pa^{-1})
R- 10	0.246 ± 0.038	0.053 ± 0.015
R- 20	0.261 ± 0.017	0.083 ± 0.022
R- 40	0.643 ± 0.040	0.32 ± 0.065
R- 60	1.19 ± 0.015	0.72 ± 0.080
R- 90	1.73 ± 0.075	0.88 ± 0.123
R-240	17.9 ± 2.25	12.1 ± 3.24

Figure 3-4 shows the molecular weight dependence of η_0 for ring PSs, compared with the linear ones. In addition to our data, the data for two highly-purified ring PSs reported by Kapnistos et al.[3] as well as those for linear PSs reported by other groups were also added to this figure. The details of the data by other groups were summarized in ref. 1. First of all in Figure 3-4, all rings exhibit clearly lower viscosities than the linear counterparts in the entire molecular weight range. Moreover, rings show different molecular weight dependence from linear chains, i.e., η_0 for rings increase proportional to the molecular weights, $\eta_0 \sim M_w^{1.0}$ for M_w up to 90 kg/mol, which is approximately five times larger than the entanglement molecular weight M_e (= 18.0 kg/mol for linear PSs). This result suggests that the ring PSs whose molecular weights are smaller than $5M_e$ apparently show the unentangled Rouse ring like behavior.[4-7] In contrast, when the molecular weights are larger than $5M_e$, they show a drastic deviation from the dependence of the

Rouse-like mode. In fact, R-240 in this study exhibits almost ten times larger η_0 than the Rouse prediction. This result strongly suggests that this large ring generates some intermolecular interactions, which is consistent with the result of comparison of the dynamic moduli in Figure 3-3.

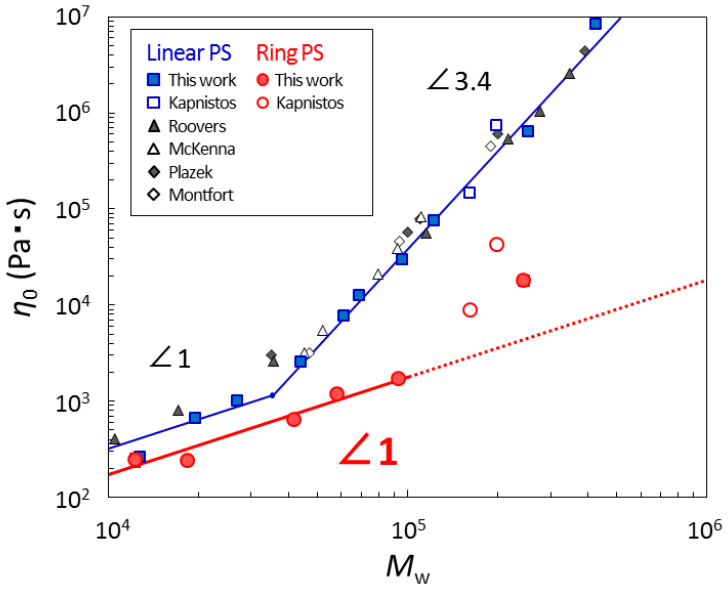

Figure 3-4. Molecular weight dependence of η_0 for ring PSs, compared with linear PSs at T_{ref} = 160 °C. Details of the data reported by other groups are summarized in ref. 1. Reprinted with permission from ref. 1.

Figure 3-5 shows the molecular weight dependence of J_e for ring PSs, compared with the linear ones. Regarding the linear molecules, J_e increase in proportional to the increase of M_w ($J_e \sim M_w^{1.0}$) up to $6M_e$, while they have a constant value ($J_e \approx 1.2 \times 10^{-5}$ Pa^{-1}) at above $6M_e$. In contrast, rings apparently show different dependence from linear chains, and their dependence can be divided into three parts. (i) In a small M_w region (M_w < 20 kg/mol), rings have approximately half J_e values of the linear counterparts. In the Rouse ring prediction, J_e for rings should be half of that for linear counterparts,[4-7] and therefore they apparently behave like Rouse rings. (ii) In an

intermediate M_w region ($40 \leq M_w \leq 90$ kg/mol), they show similar J_e to the linear ones. The viscosities are in good agreement with the Rouse ring prediction, while their J_e are not consistent with the model. (iii) The largest ring, R-240, shows an obviously high J_e, i.e., almost 10 times larger J_e than the linear counterparts. This result also indicates that this large ring generates some intermolecular interactions, which is probably much broader relaxation mode distribution and more cooperatively than those for the linear chains.

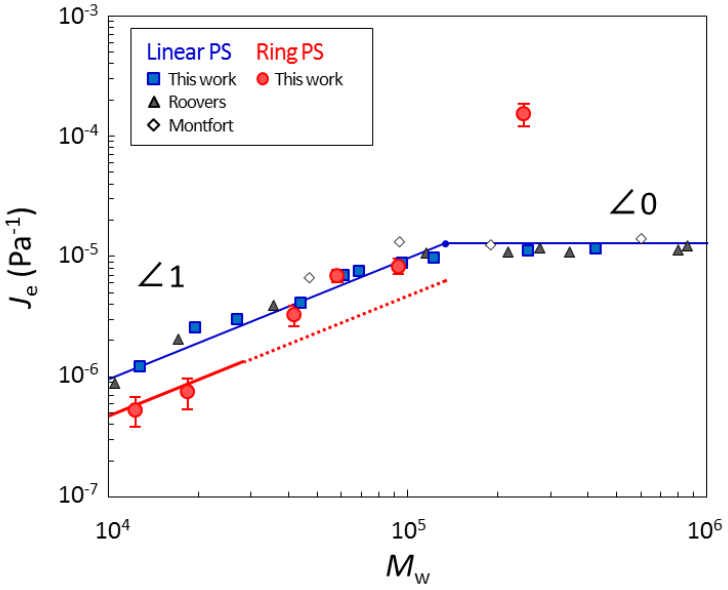

Figure 3-5. Molecular weight dependence of J_e for ring PSs, compared with linear PSs at T_{ref} = 160 °C. Details of the data reported by other groups are summarized in ref. 1. Reprinted with permission from ref. 1.

From the above, it has been found that both η_0 and J_e for ring polymers strongly depend on their molecular weights, and that there are some inconsistencies. In terms of η_0 and J_e, small rings ($M_w \leq M_e$) apparently follow the Rouse ring prediction, while large rings ($2M_e \leq M_w$) show some disagreements with the model. In contrast, the dynamic moduli for rings with the moderate molecular weights ($2M_e \leq M_w \leq 5M_e$) apparently follow the Rouse ring model, while other rings,

i.e., both small and large rings, show a discrepancy between experimental and predicted data. Basically, there is no necessity that the Rouse ring model can be applied to the ring chains in a whole range of the molecular weights because their chain conformation is not guaranteed to follow the Gaussian distribution. To elucidate the chain relaxation mechanisms of ring polymers accurately, further investigations including both experimental and theoretical aspects are necessary.

3.5. Conclusions

In this chapter, the viscoelastic properties of highly-purified ring PSs with wide molecular weight range were carefully investigated. All rings adopted in this study exhibit no rubbery plateau and faster terminal relaxation than the linear counterparts. The dynamic moduli for rings experimentally obtained were compared with those for the Rouse ring model. Rings with moderate molecular weights, $2M_e \leq M_w \leq 5M_e$, are in good agreement with the predictions, while the other rings with both small and large molecular weights exhibit discrepancy between experimental and calculated data. Moreover, it turned out to be clear that two rheological parameters, i.e., η_0 and J_e for rings strongly depend on their molecular weights. The small rings with M_w of $M_w \leq M_e$ give the Rouse model like behavior, although there is no necessity of agreement. Rings with moderate M_w ($2M_e \leq M_w \leq 5M_e$) show η_0 supported by the Rouse ring prediction, but reveal J_e of inconsistency with the model. The largest ring with M_w of $5M_e < M_w$ exhibits clearly larger η_0 and J_e than the predicted values by the model, suggesting that some intermolecular interactions are generated.

3.6. References

1. Doi, Y.; Matsubara, K.; Ohta, Y.; Nakano, T.; Kawaguchi, D.; Takahashi, Y.; Takano, A.; Matsushita, Y. *Macromolecules* **2015**, *48*, 3140-3147.
2. McLeish, T. C. B. *Science* **2002**, *297*, 2005-2006.
3. Kapnistos, M.; Lang, M.; Vlassopoulos, D.; Pyckhout-Hintzen, W.; Richter, D.; Cho, D.; Chang, T.; Rubinstein, M. *Nat. Mater.* **2008**, *7*, 997-1002.
4. Rouse, P. E. *J. Chem. Phys.* **1953**, *21*, 1272-1280.
5. Wedgewood, L. E.; Ostrov, D. N.; Bird, R. B. *J. Non-Newtonian Fluid Mech.* **1991**, *40*, 119-139.
6. Watanabe, H.; Inoue, T.; Matsumiya, Y. *Macromolecules* **2006**, *39*, 5149-5426.
7. Tsolou, G.; Stratikis, N.; Baig, C.; Stephanou, P. S.; Mavrantzas, V. G. *Macromolecules* **2010**, *43*, 10692-10713.
8. Ferry, J. D. *Viscoelastic Properties of Polymers*, 3rd ed.; Wiley: New York, 1995.
9. Zoller, P.; Walsh, D. (Ed.) *Standard Pressure-Volume-Temperature Data for Polymers*; Technomic Publishing Co.: New York, 1995.
10. Santangelo, P. G.; Roland, C. M.; Chang, T.; cho, D.; Roovers, J. *Macromolecules* **2001**, *34*, 9002-9005.
11. Kawaguchi, D.; Ohta, Y.; Takano, A.; Matsushita, Y. *Macromolecules* **2012**, *45*, 6748-6752.

Chapter 4

Viscoelastic Properties of Tadpole-Shaped Polystyrenes

Adapted with permission from
Doi, Y. et al. *Macromolecules* **2015**, *48*, 8667-8674.[1]

Abstract: Viscoelastic properties of a series of highly-purified tadpole-shaped polystyrene (PS) samples having a common ring with M_w of 59.8 kg/mol and linear tails with three different lengths, M_w of 27.1, 68.9 and 122 kg/mol, respectively, were investigated. All tadpole samples revealed a rubbery plateau and remarkably slower terminal relaxation than the component ring and linear chains and also than the ring/linear blends. These results suggest that the tadpole chains spontaneously generate characteristic interactions such as an intermolecular ring-linear penetration. Moreover, the molecular weight dependence of two rheological parameters, i.e., the zero-shear viscosity, η_0, and the steady-state recoverable compliance, J_e, was discussed. Tadpole samples exhibited drastic viscosity enhancement compared with the simple linear chains when η_0 were plotted against their total molecular weight, $M_{w,total}$. Moreover, they revealed similar molecular weight dependence to the star polymers when η_0 data were plotted against the molecular weight of a tail chain, $M_{w,tail}$, for tadpoles and that of one arm, $M_{w,arm}$, for stars. The molecular weight dependence of J_e was also similar to that of stars instead of linear chains. These results strongly suggest that the relaxation mechanism of tadpoles is similar to that of star polymers, being well understood by the arm retraction model. These characteristic rheological properties of tadpoles must be originated from their unique architecture where a ring and a linear chain are introduced into one molecule.

4.1. Introduction

Not only simple ring polymers, but also ring/linear blends are an intriguing subject of polymer dynamics. The rheological properties of ring/linear blends were recently investigated by both experiments[2] and computer simulations.[3] It was found that the dynamics of rings is very sensitive to the presence of linear chains, i.e., the ring sample exhibited a rubbery plateau when only less than a few percent of linear contaminations was included, and it revealed larger viscosity than the simple linear chain when substantial amount of linear chains are added to rings. These results strongly suggest that a new type of intermolecular entanglement i.e., ring-linear penetration spontaneously occur.

Tadpole-shaped polymers have a unique chain architecture, where one or two linear chains are attached on a ring. They are expected to show some characteristic viscoelastic properties originated from the intermolecular ring-linear penetrations in addition to the effects of connectivity of a ring and linear chains. However, there are no examples of accurate investigation of rheological properties for tadpole-shaped polymers until now.

In this chapter, viscoelastic properties of a series of highly-purified tadpole-shaped polystyrene (PS) samples having a common ring and linear tails with three different lengths were investigated. To elucidate the relaxation mechanism of the tadpole molecules, their dynamic moduli were compared with those for the component ring and linear chains and also the ring/linear blends. Moreover, the molecular weight dependence of the zero-shear viscosities, η_0, and the steady-state recoverable compliances, J_e, of the tadpoles was evaluated and discussed.

4.2. Experimental

The molecular characteristics of a series of tadpole-shaped PSs are summarized in Table 4-1. Viscoelastic properties of tadpole-shaped polymers were evaluated in the same conditions as described in Chapter 3.

Table 4-1. Molecular characteristics of a series of tadpole-shaped PSs

Samples	$10^{-3}M_w$ [a]	M_w/M_n [b]	$10^{-3}M_{w,tail}$ [a]	$M_w/M_{n,tail}$ [b]	Purity [c]
R-60	59.8	1.02	-	-	99.9
S-60/30	86.8	1.02	27.1	1.02	99.3
T-60/30	114	1.02			99.5
S-60/70	130	1.01	68.9	1.02	99.6
T-60/70	192	1.01			99.6
S-60/120	183	1.02	122	1.03	99.1
T-60/120	300	1.02			99.7

Estimated from [a]SEC-MALS, [b]SEC and [c]IC measurements

4.3. Results and Discussion

Figure 4-1 shows the master curves of $G'(\omega)$ and $G''(\omega)$ for (a), (b) tadpole-60/30, (c), (d) 60/70 and (e), (f) 60/120 series, while Figure 4-2 shows the temperature dependence of the horizontal shift factors a_T for tadpole PSs. First of all in Figure 4-1 and 4-2, the time-temperature superposition can be hold for all tadpole samples in this study, and a_T have almost similar dependence to those for linear PS with high molecular weights. After the rheological measurements, all tadpole samples were confirmed to be unbroken.

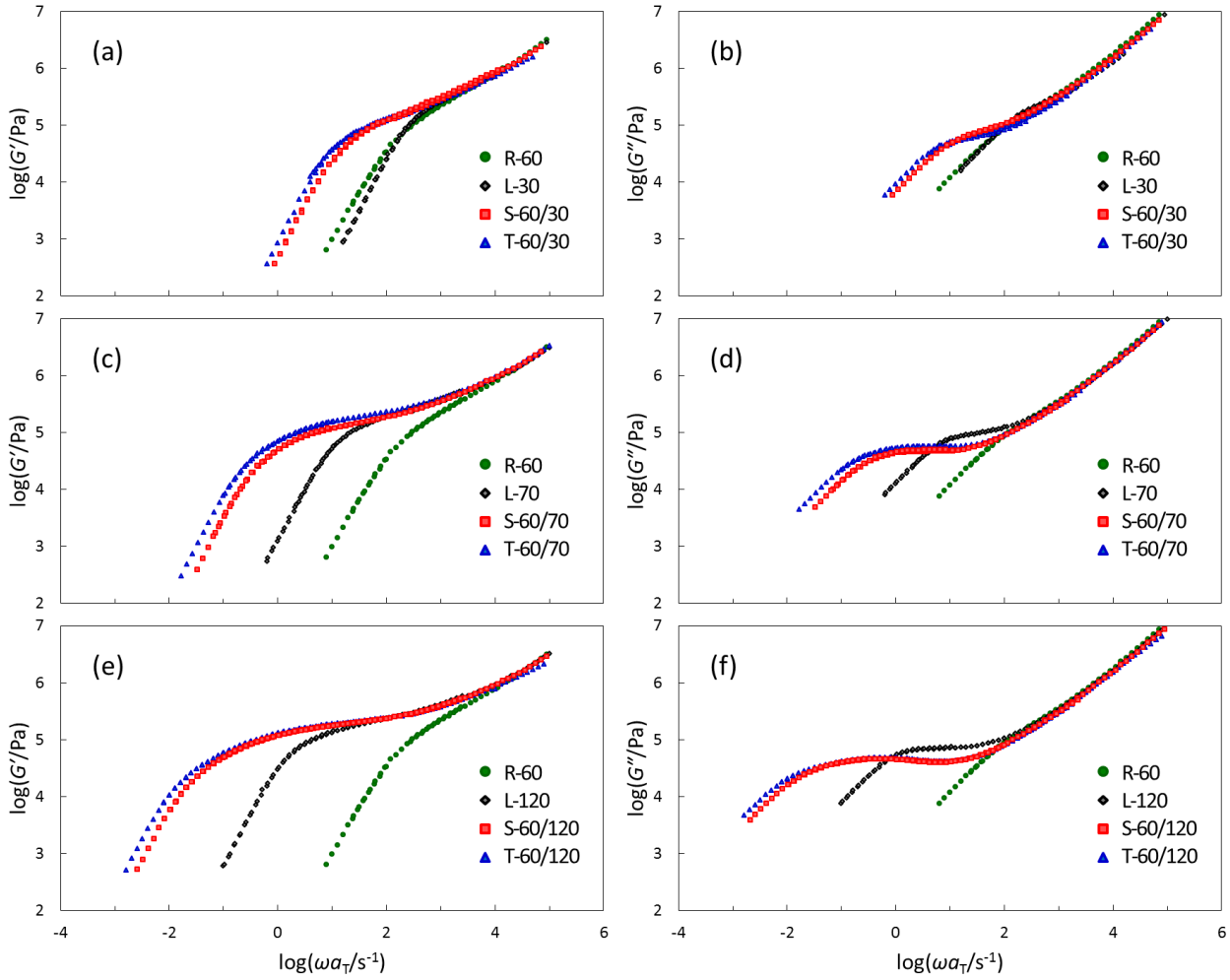

Figure 4-1. Master curves of G' and G'' for tadpole PSs compared with those for the component ring and linear PSs at T_{ref} = 160 °C: (a), (b) tadpole-60/30, (c), (d) 60/70, (e), (f) 60/120 series. Reprinted with permission from ref. 1.

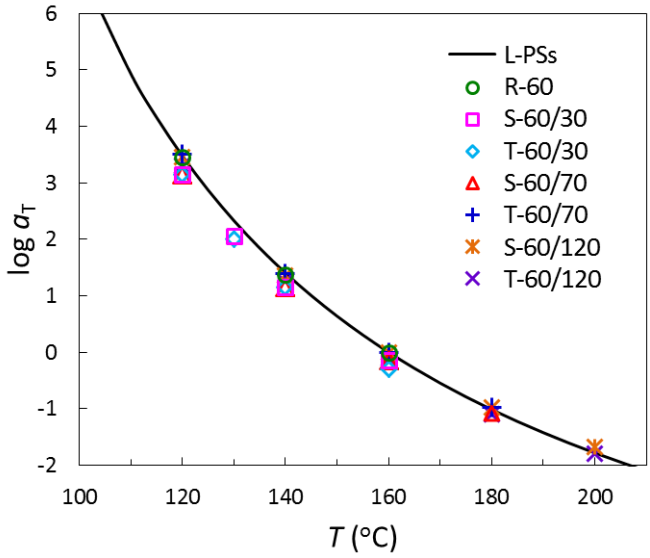

Figure 4-2. Temperature dependence of the horizontal shift factors a_T for (a) linear and (b) ring PSs at T_{ref} = 160 °C. Solid curves indicate the T dependence of a_T for long linear PSs (M_w > 40 kg/mol). Reprinted with permission from ref. 1.

In Figure 4-1, the dynamic moduli G^* in high ω regime for all tadpole PSs are in accordance with those for linear PSs, suggesting that the tadpoles have essentially the same viscoelastic segment size as the linear chains. Moreover, all tadpoles in this study exhibit a rubbery plateau and remarkably slower terminal relaxation than their component ring and linear chains. All three twin-tail tadpoles exhibit slightly slower terminal relaxations than the corresponding single-tail ones, although this difference may not be essential.

From the master curves in Figure 4-1, the zero-shear viscosities, η_0, and the steady-state recoverable compliances, J_e, for tadpole samples at T_{ref} = 160 °C were estimated in the same manner as chapter 3, and summarized in Table 4-1. To elucidate the relaxation mechanisms of the tadpole chains, the molecular weight dependence of these parameters is discussed in detail later. The plateau moduli, G_N^0, for tadpoles were determined from the G' values where the loss tangent (tan δ) has a minimum, and they are also summarized in Table 4-2.

Table 4-2. Rheological parameters, η_0 and J_e, for tadpole PSs at T_{ref} = 160 °C

Samples	$\eta_0 \times 10^{-3}$ (Pa·sec)	$J_e \times 10^5$ (Pa^{-1})	$G_N^0 \times 10^{-5}$ (Pa)
R- 60	1.19 ± 0.01	0.69 ± 0.08	-
L-30	1.00 ± 0.02	0.30 ± 0.02	-
S-60/30	6.45 ± 0.16	1.02 ± 0.01	1.38
T-60/30	9.33 ± 0.17	1.01 ± 0.05	1.34
L-70	12.5 ± 0.1	0.71 ± 0.03	2.06
S-60/70	149 ± 3.1	1.65 ± 0.03	1.36
T-60/70	260 ± 7.0	1.52 ± 0.01	1.80
L-120	75.0 ± 3.2	0.96 ± 0.09	2.01
S-60/120	1820 ± 63	2.21 ± 0.04	1.78
T-60/120	2830 ± 93	2.38 ± 0.11	1.90

The G_N^0 values for two linear tails, L-70 and L-120, are approximately 2.0×10^5 Pa, while G_N^0 for tadpoles are relatively smaller than those for the linear ones and reveal weak molecular weight dependence. For tadpoles with short tails, their G_N^0 are approximately 70% of those for linear PSs, which may be originated from the insufficient formation of entangled networks due to the shortness of linear tail. In contrast, the tadpoles with long tails have almost similar G_N^0 values to the linear chains, suggesting that they form well-entangled network and their entanglement density is not much different from that of linear chains. From these results, the ring part as well as the linear part of tadpoles is considered to contribute to the formation of the entanglement networks. In other words, tadpole chains spontaneously form the intermolecular ring-linear

penetrations as schematically illustrated in Figure 4-3. This is because if the ring part of the tadpoles is not incorporated in the entanglements but just acts like diluents, their plateau moduli should considerably decrease.

Figure 4-3. Schematic illustration of the intermolecular ring-linear penetration of single-tail tadpole molecules. Reprinted with permission from ref. 1.

To examine the effect of the tadpole-shaped architecture on their dynamics, the rheological properties of tadpoles with those of the ring/linear blends are compared. In this study, two blend samples, R-60/L-70 and R-60/L-120, were prepared with the ratio of 50/50 and 33/67 mol %, which are corresponding to the molar ratio for single-tail and twin-tail, respectively. Figure 4-4 shows the master curves of G' and G'' for (a), (b) R-60/L-70 and (c), (d) R-60/L-120 blends, being compared with the corresponding tadpoles. In this figure, the rheological spectra for the ring/linear blends almost completely overlapped with those for the simple linear chains in a whole ω regime. The rheological parameters, η_0, J_e and G_N^0, for the blends were estimated from Figure 4-4 and summarized in Table 4-3. Both η_0 and J_e for the blends do not much differ from those for the simple linear chains. The moduli, G_N^0 for the blends are slightly lower than those for the linear chains and are close to those for tadpoles. These results imply that the intermolecular ring-linear penetrations occur also in the ring/linear blend system. Consequently, the tadpole chains relax much slower than the corresponding ring/linear blends. This suggests that the connection between a ring and a linear chain in one molecule induces a drastic change in the chain motion. The linear chain in the ring/linear blends can basically follow the reptation model

as with the simple linear chain. In contrast, the motion of the linear tail on tadpoles is restricted due to the existence of the ring on a chain end of the tail, which drastically delays its motion.

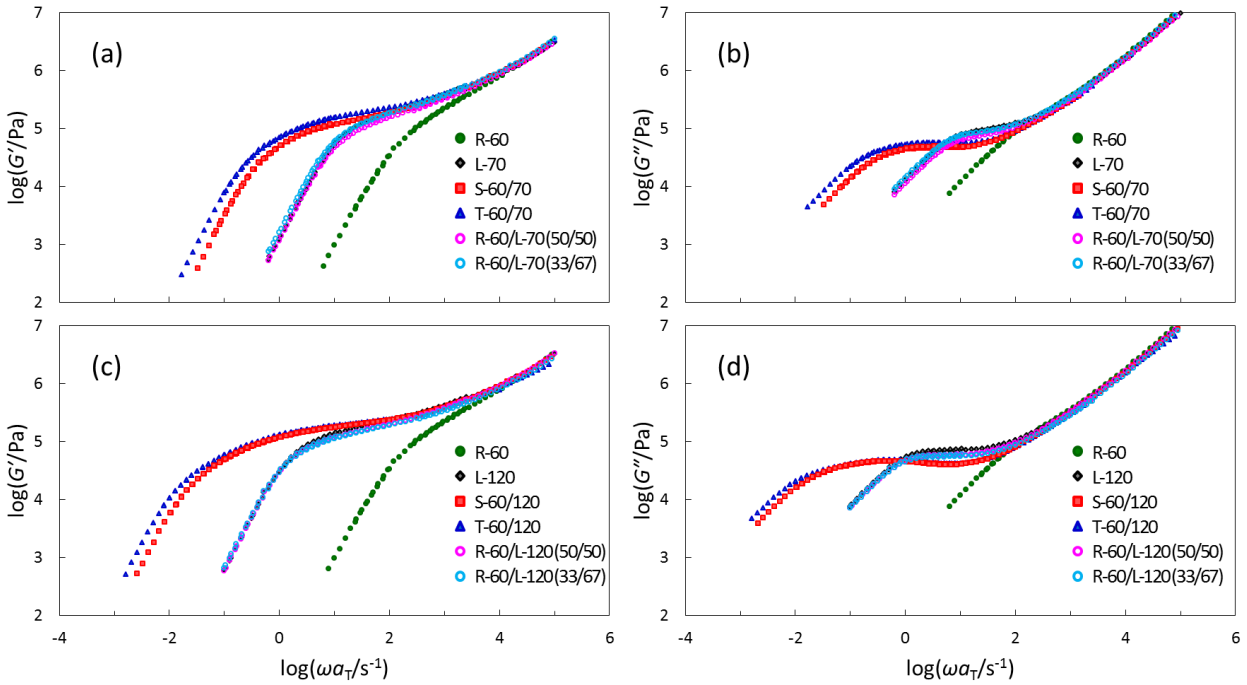

Figure 4-4. Comparison of the dynamic moduli, G' and G'', for tadpole PSs and the ring/linear PS blends at T_{ref} = 160 °C: (a), (b) tadpole-60/70 and R-60/L-70 blends, (c), (d) tadpole-60/120 and R-60/L120 blends. Reprinted with permission from ref. 1.

Table 4-3. Rheological parameters, η_0 and J_e, for the ring/linear PS blends at T_{ref} = 160 °C

Samples	$\eta_0 \times 10^{-3}$ (Pa·sec)	$J_e \times 10^5$ (Pa^{-1})	$G_N^0 \times 10^{-5}$ (Pa)
L-70	12.5 ± 0.1	0.71 ± 0.03	2.06
R-60/L-70 (50/50)	11.7 ± 0.1	0.89 ± 0.02	1.49
R-60/L-70 (33/67)	14.6 ± 0.5	0.82 ± 0.05	1.78
L-120	75.0 ± 3.2	0.96 ± 0.09	2.01
R-60/L-120 (50/50)	73.2 ± 1.1	1.08 ± 0.05	1.64
R-60/L-120 (33/67)	77.5 ± 2.3	1.14 ± 0.08	1.57

To elucidate the relaxation mechanism of tadpole chains, the molecular weight dependence of two rheological parameters, η_0 and J_e, for tadpoles at T_{ref} = 160 ^oC was discussed. In this study, these parameters were treated in two ways i.e., a function of (i) the total molecular weight ($M_{w,total}$) and (ii) the molecular weight of a linear tail of tadpoles ($M_{w,tail}$). The data were compared with those for linear, ring and star PSs. The data for linear and ring PSs were obtained from ref. 4, which includes old data reported by several groups, while those for 4-arm and 6-arm star PSs were used from the report by Graessley and Roovers in ref. 5. The reason for choosing star polymers as a reference is that they have some similarities with the tadpoles, i.e., both star and tadpole polymers have a single branch point in their structures, and their viscoelastic properties do not sensitively depend on the number of tails and arms.

Figure 4-5(a) shows η_0 for tadpole PSs plotted against their total molecular weight in double-logarithmic scales. In this figure, both single-tails and twin-tails exhibit strong molecular weight dependence, i.e., drastic viscosity enhancement compared with the simple linear polymers in the same molecular weight range. This implies that the relaxation mechanism of the tadpoles is totally different from that of simple linear chains. This remarkable result must be an intrinsic feature of the present tadpole-type molecules, each of which includes a ring and a tail chain unit in the architecture. In Figure 4-3(b), η_0 of tadpole PSs are plotted against the molecular weight of a linear tail chain. In the same way, η_0 of 4-arm and 6-arm star PSs are plotted against the molecular weight of one arm, $M_{w,arm}$. Interestingly, the data points of tadpoles stay on the exponential curve of η_0 for the stars. This result strongly suggests that the relaxation mechanism of tadpoles in this molecular weight range is similar to that of star polymers, whose dynamical motion being understood by the arm retraction model.[6-8]

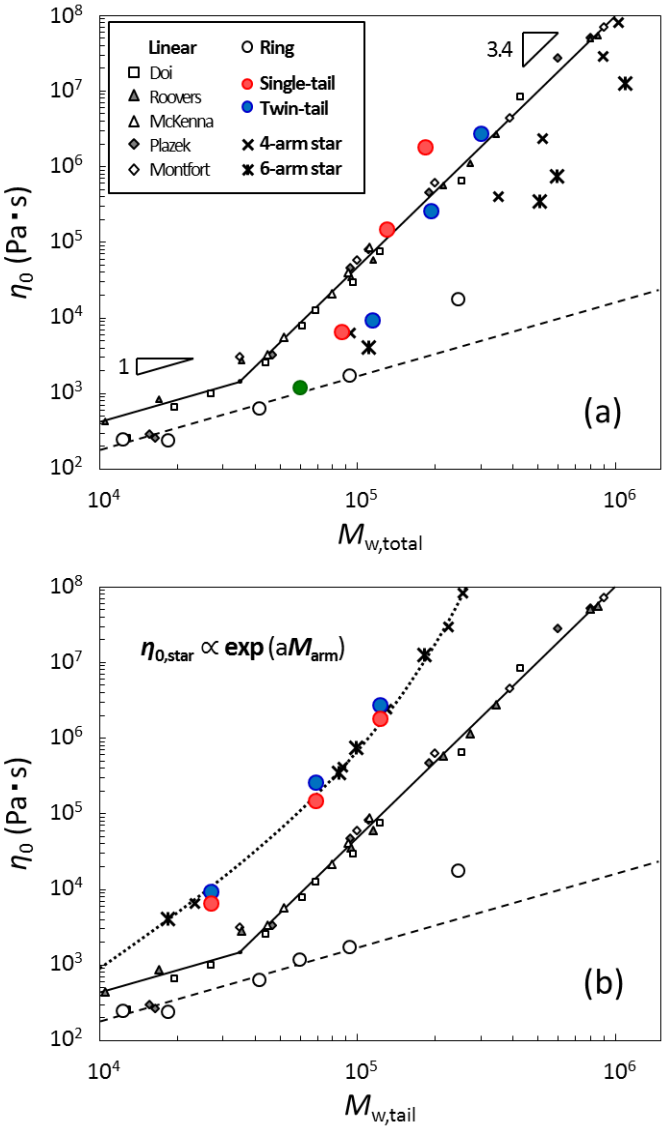

Figure 4-5. Double-logarithmic plots of η_0 versus (a) $M_{w,total}$ and (b) $M_{w,tail}$ for tadpole PSs at T_{ref} = 160 ^{o}C. The data are compared with linears, rings and 4-arm and 6-arm star PSs. The details of this figure are described in ref. 1 and 4. Reprinted with permission from ref. 1.

Figure 4-6(a) and (b) show J_e for tadpoles plotted against $M_{w,total}$ and $M_{w,tail}$, respectively. In Figure 4-6(a), J_e for tadpoles keep increasing with increase of the tail length. In fact, tadpole-60/70 and -60/120 show clearly larger J_e values than the linear polymers. In Figure 4-6(b), the tadpole-60/70 and 60/120 reveal similar J_e values to the corresponding stars, while tadpoles-60/30 exhibit evidently larger J_e than the corresponding stars. This is because tadpoles

have a ring chain in their architecture, and its contribution is not negligible (the ring R-60 itself has $J_e = 0.69 \times 10^{-5}$ Pa^{-1}) when linear tail chains become short.

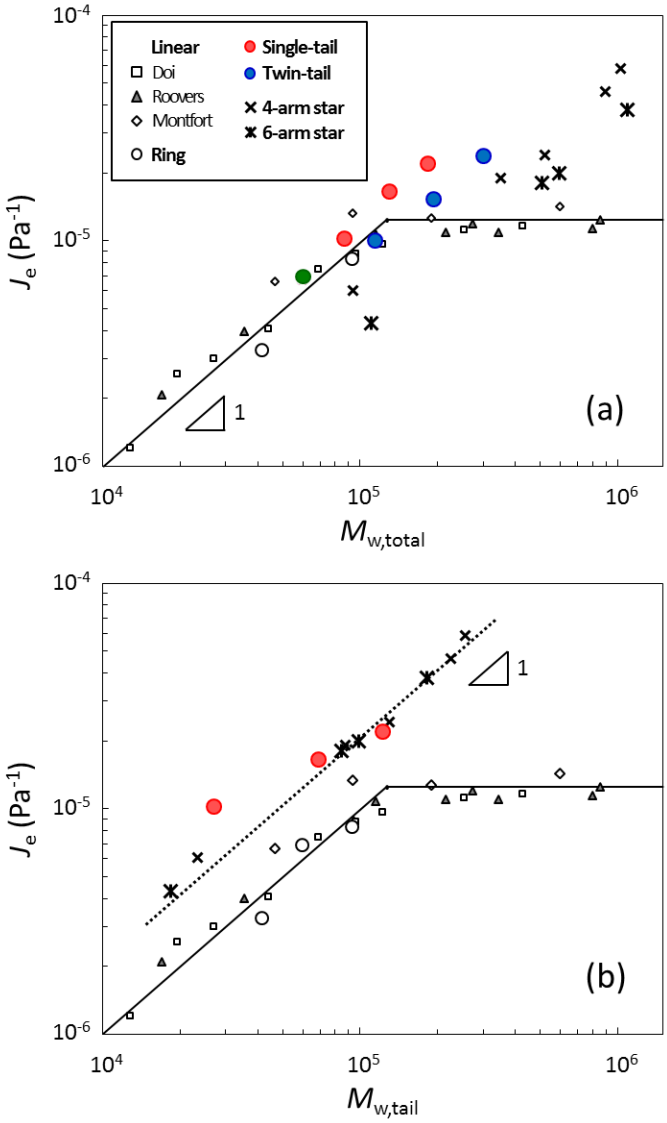

Figure 4-6. Double-logarithmic plots of J_e versus (a) $M_{w,total}$ and (b) $M_{w,tail}$ of tadpole PSs at T_{ref} = 160 ^oC. The data are compared with linears, rings and 4-arm and 6-arm star PSs. The details of this figure are described in ref. 1 and 2. Reprinted with permission from ref. 1.

To confirm the similarity between the stars and tadpoles, their dynamic moduli in a whole ω regime were directly compared. A four-arm star PS sample, S141A ($M_{w,total}$ = 521, $M_{w,arm}$ = 130

kg/mol) was chosen as a reference sample from the previous data reported by Graessley et al. to compare its spectra with those for our tadpole sample, S-60/120 ($M_{w,total}$ = 183, $M_{w,arm}$ = 122 kg/mol), because the molecular weight of one arm of the star is close to that of a tail of the present tadpole molecule. Figure 4-7 shows a comparison of the dynamic moduli for S-60/120 and S-141A at T_{ref} = 160 °C. The master curves of S141A are almost perfectly overlapped with those for S-60/120 in a whole ω regime adopted. A small difference is observed in the terminal region, i.e., the terminal relaxation of the star is a little slower than that of the tadpole, which is probably due to the small difference in between $M_{w,arm}$ and $M_{w,tail}$. Except for this small difference, the result in Figure 4-7 strongly supports that the relaxation mechanism of tadpole chains in this molecular weight range is in the same manner as that of star polymers.

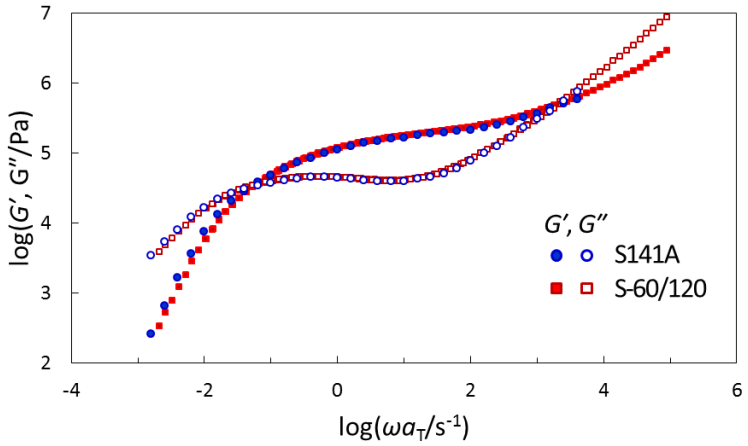

Figure 4-7. Comparison of the dynamic moduli, G' and G'', for the single-tail PS, S-60/120 and the four-arm star PS, S141A at T_{ref} = 160 °C. Reprinted with permission from ref. 1.

Now there is an open question why the tadpole chains follow the relaxation mechanism like star polymers. This is probably due to the occurrence of the spontaneous ring-linear penetration between tadpole chains as schematically illustrated in Figure 4-3, which induces remarkable restriction of the motion for the ring part as well as the chain end of a linear tail attached on the

ring. In other word, if the ring part of tadpoles does not concern any intermolecular interactions, their characteristic star-like relaxation behavior would be expressed. Figure 4-7 shows a good evidence to support a hypothesis for the following reason. The tadpole sample, S-60/120, may be regarded as an asymmetric three-arm star polymer with two short arms ($M_{w,short}$ = 59.8/2 = 29.9 kg/mol) and one long arm ($M_{w,long}$ = 122 kg/mol), if a ring part of the tadpole is cut into two chains with the same length and they do not interact with each other due to the small molecular weight. In this case, the asymmetric star should show much faster relaxation than the symmetric stars with the long arms, which corresponds to S141A in Figure 4-7, because two short arms of the asymmetric star can relax much faster than the other long arm and they dilute the remaining entanglements. Such behavior of asymmetric stars was already revealed experimentally by several groups.[9,10] If a ring part of the tadpole S-60/120 does not show any intermolecular interactions like two short arm chains of the asymmetric star, this molecule should relax faster than the symmetric star. Nevertheless, S-60/120 exhibits almost the same rheological spectra with S141A as mentioned above. This result supports that the intermolecular ring-linear penetration is evidently generated for tadpole chains to exhibit their star-like relaxation. Moreover, it can be considered that the relaxation of the ring part threaded by other linear tails occurs only when the ring is released from the threading. In other words, the relaxation of ring part occurs simultaneously with that of the linear tails.

4.4. Conclusions

In this chapter, the viscoelastic properties of a series of highly-purified tadpole-shaped PSs were investigated. It has been found that all tadpole samples used in this study exhibited a rubbery plateau and slower terminal relaxation than the component ring and linear chains and

also than the ring/linear blends. These results suggest that the tadpole chains spontaneously generate characteristic interactions such as an intermolecular ring-linear penetration. Moreover, the molecular weight dependence of η_0 for tadpoles was highly interesting, i.e., they exhibited a drastic viscosity enhancement compared with the simple linear chains when η_0 data were plotted against $M_{w,total}$, while they revealed similar molecular weight dependence to the star polymers when η_0 were plotted against $M_{w,tail}$ and $M_{w,arm}$. The molecular weight dependence of J_e was also similar to that of stars instead of linear polymers. From these results, the relaxation mechanism of tadpole chains is considered to be taken place in the same manner as that of star polymers, which can be described by the arm retraction model, coupled with the intermolecular ring-linear penetrations of tadpole chains.

4.5. References

1. Doi, Y.; Takano, A.; Takahashi, Y.; Matsushita, Y. *Macromolecules* **2015**, *48*, 8667-8674.
2. Kapnistos, M.; Lang, M.; Vlassopoulos, D.; Pyckhout-Hintzen, W.; Richter, D.; Cho, D.; Chang, T.; Rubinstein, M. *Nat. Mater.* **2008**, *7*, 997-1002.
3. Halverson, J. D.; Grest, G. S.; Grosberg, A. Y.; Kremer, K.: *Phys. Rev. Lett.* **2012**, *108*, 038301.
4. Doi, Y.; Matsubara, K.; Ohta, Y.; Nakano, T.; Kawaguchi, D.; Takahashi, Y.; Takano, A.; Matsushita, Y. *Macromolecules* **2015**, *48*, 3140-3147.
5. Graessley, W. W.; Roovers, J. *Macromolecules* **1979**, *12*, 959-965.
6. de Gennes, P. G. *J. Phys. (Paris)* **1975**, *36*, 1199-1203.
7. Doi, M.; Kuzuu, N. Y. *J. Polym. Sci., Polym. Lett. Ed.* **1980**, *18*, 775-780.
8. Milner, S.; McLeish, T. C. B. *Macromolecules* **1997**, *30*, 2159-2166.
9. Gell, C. B.; Graessley, W. W.; Efstratiadis, V.; Pitsikalis, M.; Hadjichristidis, N. *J. Polym. Sci., Part B: Polym. Phys.* **1997**, *35*, 1943-1954.
10. Frischknecht, A. L.; Milner, S. T.; Pryke, A.; Young, R. N.; Hawkins, R.; McLeish, T. C. B. *Macromolecules* **2002**, *35*, 4801-4820.

Chapter 5

Viscoelastic Properties of Comb-Shaped Ring Polystyrenes

Abstract: Viscoelastic properties of a series of comb-shaped ring polystyrene samples, named RC, with the different branch chain length were investigated. It has been found that the dynamic moduli for RC samples are mainly composed of two terms originated from the relaxation of branches and that of the backbone. Moreover, the relaxation of branches for RC samples is similar to that for the corresponding linear comb molecules, LC, while the relaxation of the backbone for RC is clearly faster than that for the LC. From these results, the difference in the backbone chain architecture directly affects the viscoelastic properties of the comb-shaped polymers. Moreover, dynamic moduli for short branch systems with no entanglements were compared with the model predictions. It has been found that the dynamic moduli experimentally obtained can be described by the simple sum of the Rouse-Ham and Rouse models when any entanglements do not occur.

5.1. Introduction

Branched polymers are conceived to reveal some unique properties based on their characteristic structures.[1,2] In a viewpoint of the polymer dynamics, they are known to exhibit hierarchical relaxation originated from their hierarchical branch structures.[3] Most of the branched polymers are composed of polymer segments with chain ends, and hence it is rare to introduce ring structure into branched polymers. Comb-shaped ring polymers are one of the models with regularly branched structure consisting of two kinds of chains, i.e., many branched chains and a ring backbone. Thus, by adopting a ring chain as a comb backbone, a new type of branched polymer can be created, which can represent the properties of both ring backbone and branched linear chains.

In this chapter, the viscoelastic properties of a series of comb-shaped ring polystyrene (PS) samples having a common ring backbone and linear branches with different lengths were evaluated in comparison with those for the linear counterparts. Their dynamic moduli obtained were compared with some model predictions.

5.2. Experimental

The molecular characteristics of a series of comb-shaped ring PS samples (RC) and their linear counterparts (LC) are summarized in Table 5-1. Viscoelastic properties of the comb-shaped samples were evaluated in the same manner as described in the previous chapters.

Table 5-1. Molecular characteristics of a series of LC and RC samples

Samples	$10^{-3}M_w$ [a]	M_w/M_n [b]	$10^{-3}M_{w,br}$ [a]	f [c]
LC-20	491	1.02	20.2	21
RC-20	434	1.03	19.2	19
LC-40	1070	1.05	41.5	24
RC-40	929	1.04	41.5	21
LC-80	1630	1.07	75.9	21
RC-80	1100	1.14	75.9	14

Estimated from [a]SEC-MALS and [b]SEC measurements. [c]f: the number of branches calculated from $f = (M_w - M_{w,bb})/M_{w,br}$.

5.3. Results and Discussion

Figure 5-1 shows the master curves of $G'(\omega)$, $G''(\omega)$ and tanδ for (a) RBB-70, (b) RC-20, (c) RC-40 and (d) RC-80, compared with the corresponding linear counterparts. In Figure 5-1(a), LBB-70 exhibits a clear rubbery plateau, while RBB-70 exhibits no rubbery plateau, even though they have the same molecular weights. The similar result for trivial rings was already reported in chapter 3.

In Figure 5-1(b)-(d), it was found that both LC and RC samples exhibit slower terminal relaxation as the branch chains become longer. Moreover, three LC samples reveal a common characteristic viscoelastic feature: loss tangents (tanδ) for LC samples show a minimum and an inflection point. This suggests that the LC samples have two distinctive relaxation modes, where the multiple branch chains relax fast and the diluted backbone relaxes later. Such behavior for comb-shaped polymers is already known well.[3-6] The minimum of tanδ for RC samples is observed at similar ω position with that for the corresponding LC, suggesting that the relaxation behavior of branch chains is basically the same between LC and RC. This is probably reasonable because the number and length of branch chains of RC samples are similar to those of the corresponding LC. In contrast, a clear difference is observed in tanδ of LC and RC in low ω regime, i.e., the terminal relaxation of RC samples clearly is faster than that of the corresponding LC samples and the relaxation intensity of the ring backbone in RC samples is too weak to be seen in the tanδ spectra. From the above, the difference in the backbone chain architecture directly affects the viscoelastic properties of the comb-shaped polymers.

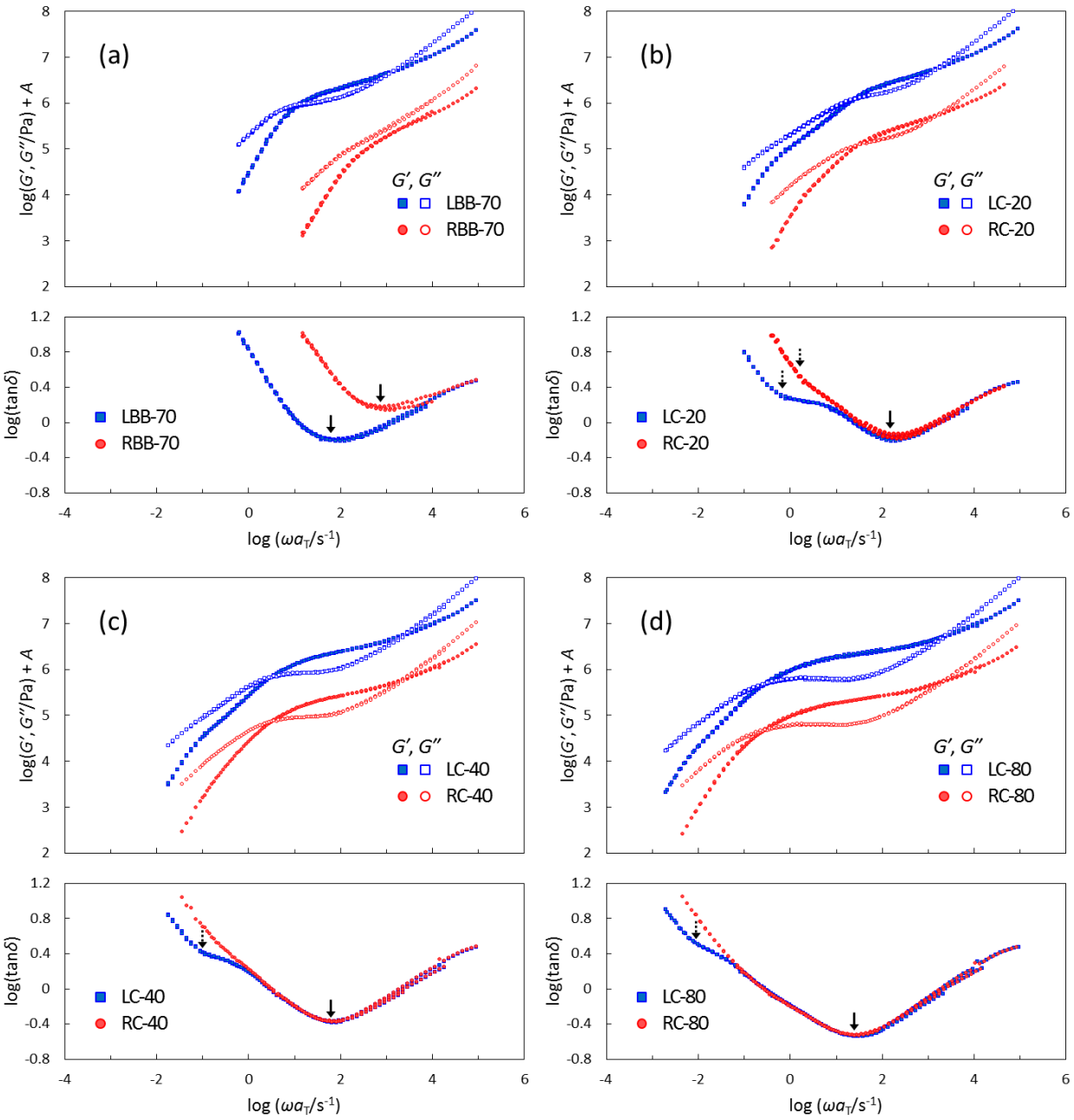

Figure 5-1. Master curves of G' and G'' (top), and tanδ (bottom) for (a) RBB-70, (b) RC-20, (c) RC-40 and (d) RC-80, compared with the corresponding linear counterparts at T_{ref} = 160 ^{o}C. The solid and dotted arrows indicate the lowest and inflection points, respectively. The moduli for linear ones are vertically shifted by a factor of A = 1.

Moreover, the experimental dynamic moduli are compared with the theoretical predictions. The moduli of comb samples, $G^*_{comb}(\omega)$, may be written as a simple summation of three terms originated from the relaxation of the glassy mode, the branches and the backbone as follows:

$$G^*_{comb}(\omega) = G^*_{glass}(\omega) + G^*_{br}(\omega) + G^*_{bb}(\omega) \quad (5\text{-}1)$$

If there are not any entanglements in the systems, $G^*_{br}(\omega)$ and $G^*_{bb}(\omega)$ can be described by the Rouse-Ham and the Rouse models, respectively, as follows:[7,8]

$$G^*_{br}(\omega) = \phi_{br}\frac{\rho RT}{fM_{br}}\left\{(f-1)\sum_{k=1}^{N}\frac{i\omega\tau_{2k-1}}{1+i\omega\tau_{2k-1}} + \sum_{k=1}^{N}\frac{i\omega\tau_{2k}}{1+i\omega\tau_{2k}}\right\} \quad (5\text{-}2)$$

$$G^*_{bb}(\omega) = \phi_{bb,eff}\frac{\rho RT}{M_{bb}}\sum_{p=1}^{N}\frac{i\omega\tau_p}{1+i\omega\tau_p} \quad \textit{for linear backbones} \quad (5\text{-}3\text{-}1)$$

$$G^*_{bb}(\omega) = \phi_{bb,eff}\frac{2\rho RT}{M_{bb}}\sum_{p=1}^{N}\frac{i\omega\tau_p}{1+i\omega\tau_p} \quad \textit{for ring backbones} \quad (5\text{-}3\text{-}2)$$

where ρ is the density for PS, R is the gas constant, p is the mode number, τ_p is the pth relaxation time, Φ_{br} is the volume fraction of the branches and $\Phi_{bb,eff}$ is the effective volume fraction of the backbone (= $k \times \Phi_{bb}$). Figure 5-2(a) shows results of the theoretical prediction of the ring backbone by using eq.(5-3-2), while Figure 5-2(b) shows that of LC-20 and RC-20 by the combination of the above equations, all of which can be considered as unentangled systems. The parameters used in this prediction were summarized in Table 5-2. The contribution of the glassy mode is considered as $G''(\omega) = 10^{1.9}\omega$ for all samples.

The experimental data for both LC-20 and RC-20 shows good agreement with the theoretical predictions. Therefore, it has been found that the dynamic moduli for the comb-shaped ring

polymers with short branches without any entanglements can be described by the simple sum of the Rouse-Ham (the relaxation of branches) and Rouse models (that of the backbone).

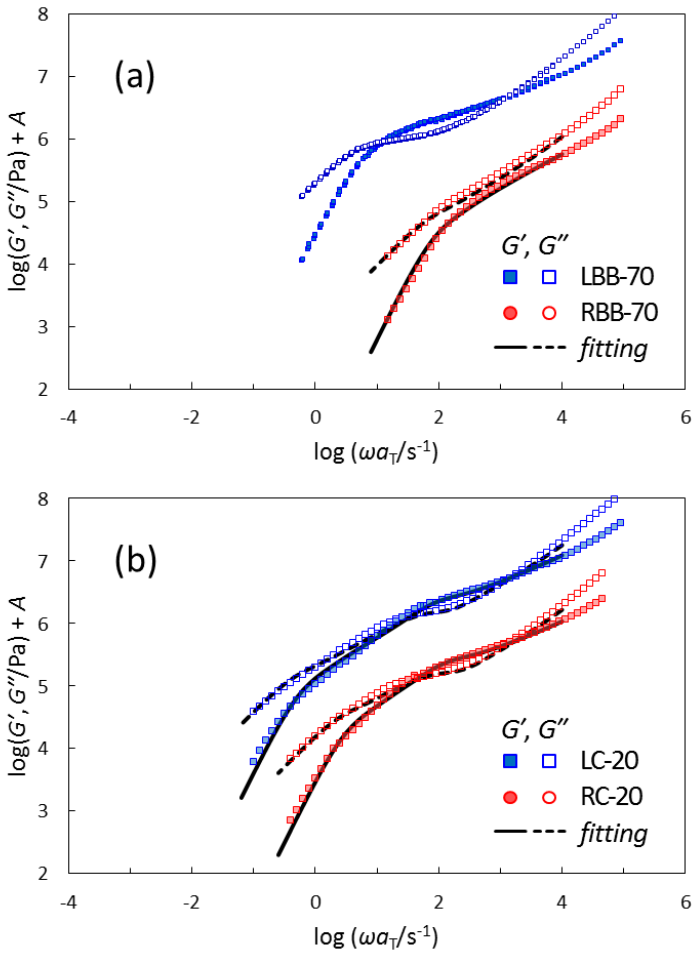

Figure 5-2. Comparison of experimental data and theoretical predictions of G' and G'' for (a) R-BB and (b) RC-20, compared with the linear counterparts at T_{ref} = 160 °C.

Table 5-2. Parameters used in the fitting in Figure 5-2

Samples	ρ (g/cm^3)	$\langle\tau_{br}\rangle_w$ (sec)	$\langle\tau_{total}\rangle_w$ (sec)	k
RBB-70	1.05	-	0.010	-
LC-20	1.05	0.016	1.62	2.0
RC-20	1.05	0.011	0.30	2.0

5.4. Conclusions

In this chapter, viscoelastic properties of a series of comb-shaped ring PS, RC, samples with the different branch chain length were investigated. It has been found that the dynamic moduli for RC are mainly composed of two terms originated from the relaxation of branches and that of the backbone. Moreover, the relaxation of branches for RC samples is similar to that for the corresponding linear counterparts, LC, while the relaxation of the backbone for RC is clearly faster than that for the LC. From these results, the difference in the backbone chain architecture directly affects the viscoelastic properties of the comb-shaped polymers. Furthermore, dynamic moduli for short branch systems with no entanglements were compared with model predictions. It has been found that the dynamic moduli experimentally obtained can be described by the simple sum of the Rouse-Ham and Rouse models when any entanglements do not occur.

5.5. References

1. Roovers, J. (ed.) *Adv. Polym. Sci.; Branched Polymers I*, vol. 142; Springer, Berlin, 1999.
2. Roovers, J. (ed.) *Adv. Polym. Sci.; Branched Polymers II*, vol. 143; Springer, Berlin, 1999.
3. McLeish, T. B. C. *Europhys. Lett.* **1988**, *6*, 511-516.
4. Roovers, J.; Graessley, W. W.; *Macromolecules* **1981**, *14*, 766-773.
5. Daniels, D. R.; McLeish, T. C. B.; Crosby, B. J.; Young, R. N.; Fernyhough, C. M. *Macromolecules* **2001**, *34*, 7025-7033.
6. Kapnistos, M.; Vlassopoulos, D.; Roovers, J.; Leal, L. G. *Macromolecules* **2005**, *38*, 7852-7862.
7. Rouse, P. E. *J. Chem. Phys.* **1953**, *21*, 1272-1280.
8. Ham, J. E. *J. Chem. Phys.* **1957**, *26*, 625-633.

Chapter 6

Viscoelastic Properties of Dumbbell-Shaped Polystyrenes

Abstract: Viscoelastic properties of a dumbbell-shaped polystyrene sample, where rings with M_w of 33.7 kg/mol were attached on both ends of a linear chain with M_w of 241 kg/mol, were investigated. It has been found that the dumbbell polymer exhibits an extremely long rubbery plateau and does not reach the terminal region within the measurement range adopted. This behavior is similar to that of cross-linked polymers, strongly suggesting that the dumbbell chains form a new type of entangled network. That is, two ring parts on a dumbbell chain were penetrated by the other chains, and hence the chain can behave as a bridge of at least two chains. A larger fraction of dumbbell molecules may participate in this mutual penetration, and consequently the whole system actually forms three-dimensional network (cf. Figure 6-4 in page 76). The characteristic viscoelastic properties mentioned above must be originated from the unique chain architecture, i.e., the target molecule has no chain ends but have one ring each on both ends.

6.1. Introduction

As mentioned in the previous chapters, polymer dynamics is closely related to the polymer chain architecture. In particular, the presence or absence of chain ends gives a significant influence, i.e., ring polymers has much less intermolecular entanglement than the corresponding linear ones.[1,2] Moreover, it has been found that ring/linear coexisting systems such as tadpole-shaped polymers[3] generate some synergetic effects of entanglements due to the intermolecular ring-linear penetrations.

Dumbbell-shaped polymer has a unique chain architecture, where rings are attached on both ends of a linear chain. Namely, this polymer has both ring and linear unit, but possesses no chain ends in its structure. Therefore, the dumbbell chain may be conceived to exhibit less entangled behavior similar to simple rings due to the absence of chain ends. In contrast, it may exhibit some intermolecular interactions such as tadpole-shaped polymers. Thus examining the rheological properties of dumbbell polymers must be important to understand further the relation between the polymer chain architecture and its dynamics.

In this chapter, the viscoelastic properties of a dumbbell-shaped polystyrene (PS) sample were investigated, and they were compared with those for its component chains.

6.2. Experimental

The molecular characteristics of two dumbbell-shaped PSs are summarized in Table 6-1. Viscoelastic properties of the comb-shaped samples were evaluated in the same manner as described in previous chapters. Since the amount of D-30/80/30 was limited (~ 5 mg), its viscoelastic properties could not be evaluated, and only those of D-30/240/30 were investigated.

Table 6-1. Molecular characteristics of dumbbell-shaped polystyrenes

Samples	$10^{-3}M_w$ [a]	$10^{-3}M_{w,ring}$ [a]	$10^{-3}M_{w,linear}$ [a]	M_w/M_n [b]	Purity [c]
D-30/80/30	147	33.7	84.0	1.01	~ 99%
D-30/240/30	301		241	1.01	~ 99%

Estimated by (a) SEC-MALS, (b) SEC and (c) IC measurements

6.3. Results and Discussion

Figure 6-1 shows the master curves of (a) $G'(\omega)$, $G''(\omega)$ and (b) tanδ for D-30/240/30, compared with those for the ring and linear components, R-30 and L-240. First of all, the moduli for the dumbbell in high ω regime (ω = 10^{-3}-10^{-5} s^{-1}) are clearly lower than those for the components, although their tanδ are in good agreement in this ω regime. This is probably because the dumbbell sample did not melt even at a high temperature (~190 ^{o}C), and therefore it did not fully cover the plates of the geometry when it was set on the rheometer. Therefore, the moduli for D-30/240/30 were vertically shifted to fit those for L-240 in high ω regime, because they are thought to be basically coincident. The result after correction is shown in Figure 6-2. The dumbbell polymer exhibits an extremely long rubbery plateau and does not reach the terminal region within the measurement range, even though its component, L-240, shows a clear terminal relaxation in the same ω regime. This behavior is like a cross-linked polymer, and the existence of two small rings attached on both ends of the long linear chain must cause it.

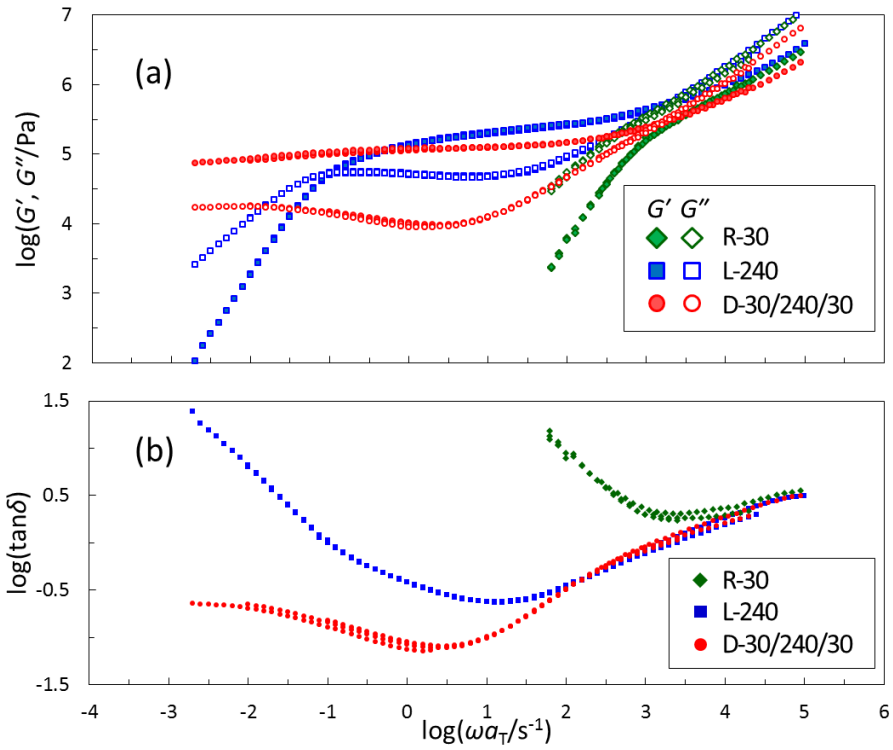

Figure 6-1. Master curves of (a) G' and G'', and (b) tanδ for dumbbell PS, D-30/240/30 (red), compared with those for the component linear and ring PS, L-240 (blue) and R-30 (green), at T_{ref} = 160 ^{o}C.

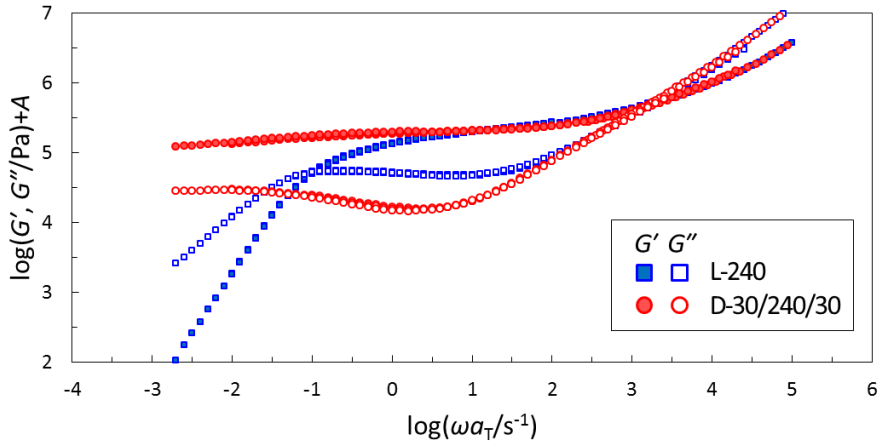

Figure 6-2. Master curves of G' and G'' for D-30/240/30 (red) compared with L-240 (blue) at T_{ref} = 160 ^{o}C. The data for D-30/240/30 is vertically shifted by a factor of A = 0.23.

After the rheological measurements, SEC measurement of D-30/240/30 was performed to check whether the chain degradations or the cross-linking occur. The result is shown in Figure 6-3. Although the peak shape becomes marginally broad, the sample is not essentially broken and cross-linked after the measurements.

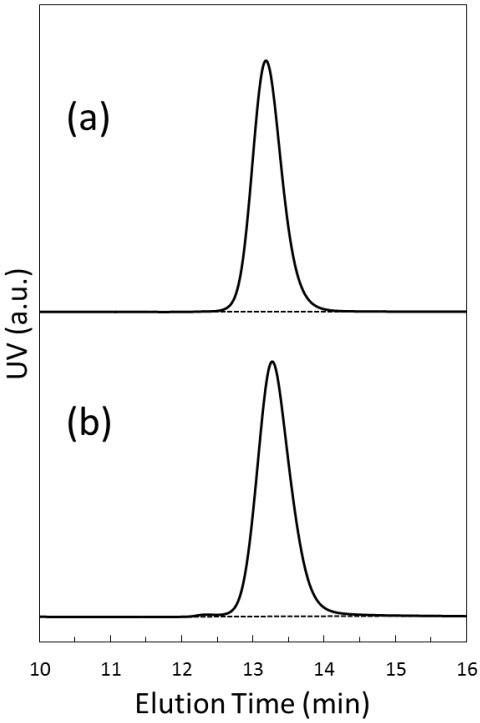

Figure 6-3. SEC chromatograms of D-30/240/30 (a) before and (b) after rheological measurements.

From the above results, this dumbbell polymer is considered to form a novel type of entanglement network, where one dumbbell chain spontaneously penetrates the ring part of other chain, and most of the chains generate this kind of penetration one after another, as schematically illustrated in Figure 6-4.

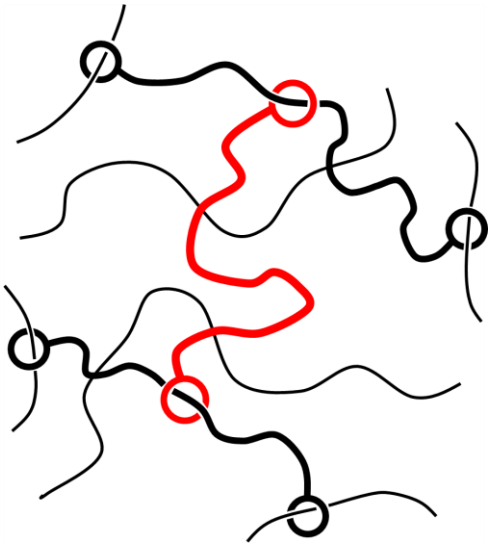

Figure 6-4. Schematic illustration of entangled dumbbell polymer network.

Now there is an open question why this dumbbell polymer forms such characteristic network. This is probably because the rings of the dumbbell polymer are more stable when they are threaded by other chains, than when they do not have any intermolecular interactions and therefore they are isolated,[1,2] in terms of the chain conformation in bulk. Lastly, it should be noted that the conformation of the dumbbell chains in bulk is completely different from that in dilute solution, where they tend to behave as a single molecule, as shown in Figure 5-6. This is another interesting topic of the dumbbell polymers.

6.4. Conclusions

In this chapter, the viscoelastic properties of a dumbbell-shaped PS, D-30/240/30 were investigated. It has been found that the dumbbell polymer exhibits an extremely long rubbery plateau and does not reach the terminal region within the measurement range adopted, which is just like cross-linked polymers. This is probably because the dumbbell chains form a new type of entangled network. That is, two ring parts on a dumbbell chain were penetrated by the other chains, and hence the chain can behave as a bridge of at least two chains. A larger fraction of dumbbell molecules may participate in this mutual penetration, and consequently the whole system actually forms three-dimensional network. Thus, it can be concluded that dumbbell polymers can exploit a possibility to generate a new type of intermolecular ring-linear interactions.

6.5. References

1. Kapnistos, M.; Lang, M.; Vlassopoulos, D.; Pyckhout-Hintzen, W.; Richter, D.; Cho, D.; Chang, T.; Rubinstein, M. *Nat. Mater.* **2008**, *7*, 997-1002.
2. Doi, Y.; Matsubara, K.; Ohta, Y.; Nakano, T.; Kawaguchi, D.; Takahashi, Y.; Takano, A.; Matsushita, Y. *Macromolecules* **2015**, *48*, 3140-3147.
3. Doi, Y.; Takano, A.; Takahashi, Y.; Matsushita, Y. *Macromolecules* **2015**, *48*, 8667-8674.
4. Arrighi, V.; Gagliardi, S.; Dagger, A. C.; Semlyen, J. A.; Higgins, J. S.; Shenton, M. J. *Macromolecules* **2004**, *37*, 8057-8065.
5. Takano, A.; Kinoshita, K.; Doi, Y.; Ohta, Y.; Matsushita, Y. unpublished data.

Chapter 7

Summary

In this thesis, ring polymers and ring-based polymers with various architectures were precisely prepared by anionic polymerizations followed by multistep HPLC fractionations, and their viscoelastic properties were carefully investigated. The relation between chain architectures having featured ring partial chains and their dynamics was extensively examined and clarified.

In chapter 1, general introduction for physical properties of polymers based on their chain architectures, especially focusing on ring polymers, was given.

In chapter 2, highly-purified three kinds of ring-based polymers, tadpole-shaped, dumbbell-shaped and comb-shaped ring polystyrenes, in addition to simple ring polymers were precisely prepared by anionic polymerizations followed by multistep HPLC fractionations. All of the samples obtained were characterized by SEC-MALS and IC measurements and were confirmed to have definite architectures with extremely high purity over 99%.

In chapter 3, the viscoelastic properties of highly-purified ring PSs with wide molecular weight range were investigated. All rings treated in this study exhibited no rubbery plateau and faster terminal relaxation than the linear counterparts. Their relaxation parameters, i.e., the zero-shear viscosities, η_0, and the steady-state recoverable compliances, J_e, strongly depend on their molecular weights, whose range can be divided into three categories, i.e., (1) small rings with M_w of $M_w \leq M_e$ apparently followed the Rouse ring model, (2) for moderate size rings with M_w of $2M_e \leq M_w \leq 5M_e$, their viscosities agreed with the model, while their compliances were inconsistent with the model, (3) the largest ring with M_w of $5M_e < M_w$ revealed sufficiently larger

η_0 and J_e values than those of the prediction, suggesting that the ring generates some additional intermolecular interactions.

In chapter 4, the viscoelastic properties of a series of highly-purified tadpole-shaped PSs were investigated. All tadpole samples adopted in this study exhibited slower terminal relaxation than the component ring and linear chains, suggesting that the tadpole chains spontaneously generate characteristic interactions such as an intermolecular ring-linear penetration. Moreover, it has been confirmed that they revealed a drastic viscosity enhancement, indicating that their relaxation mechanism is similar to that of star polymers.

In chapter 5, viscoelastic properties of a series of comb-shaped ring PSs were studied by comparing with those for the linear counterparts. All comb samples used in this study have been found to exhibit two kinds of relaxation modes, originated from the branched chains and the backbone chain. The terminal relaxation of comb-shaped rings was faster than the corresponding linear combs due to the difference in the backbone chain architecture. Moreover, the dynamic moduli of comb samples can be described by the simple sum of the Rouse-Ham and Rouse models when any entanglements do not occur.

In chapter 6, the viscoelastic properties of a dumbbell-shaped PS were investigated. The dumbbell polymer with a long middle linear chain exhibited an extremely long rubbery plateau similar to a cross-linked polymer and it did not reach the terminal region within the measurement range. This is probably because the dumbbell chains formed a new type of entanglement network, where two ring chains on a dumbbell molecule were deeply penetrated by the other chains, and hence the whole system can form three-dimensional network.

Publication List

1. "Precise Synthesis and Characterization of Tadpole-Shaped Polystyrenes with High Purity"

   Yuya Doi, Yutaka Ohta, Masahide Nakamura, Atsushi Takano, Yoshiaki Takahashi and Yushu Matsushita

   Macromolecules **2013**, *46*, 1075-1081.

2. "Melt Rheology of Ring Polystyrenes with Ultrahigh Purity"

   Yuya Doi, Kazuki Matsubara, Yutaka Ohta, Tomohiro Nakano, Daisuke Kawaguchi, Yoshiaki Takahashi, Atsushi Takano and Yushu Matsushita

   Macromolecules **2015**, *48*, 3140-3147. (Selected as ACS Editors' Choice)

3. "Melt Rheology of Tadpole-Shaped Polystyrenes"

   Yuya Doi, Atsushi Takano, Yoshiaki Takahashi and Yushu Matsushita

   Macromolecules **2015**, 48, 8667-8674. (Selected as a Cover Art)

4. "Synthesis, Characterization and Melt Rheology of Comb-Shaped Ring Polystyrenes"

   Yuya Doi, Kazuki Watanabe, Masahide Nakamura, Atsushi Takano, Yoshiaki Takahashi and Yushu Matsushita

   in preparation.

5. "Synthesis and Rheology of Dumbbell-Shaped Polystyrenes"

   Yuya Doi, Atsushi Takano, Yoshiaki Takahashi and Yushu Matsushita

   in preparation

Acknowledgements

This study was thoroughly conducted by the author during the Ph.D. course in Department of Applied Chemistry, Graduate School of Engineering, Nagoya University.

I would like to express my gratitude to my advisor, Prof. Yushu Matsushita for his passionate guidance and encouragement, as well as for providing a lot of precise opportunities to participate in conferences and to go abroad to study and research. I am thankful to Associate Prof. Atsushi Takano for his continuous support and teaching many research skills. I would thank Prof. Takahiro Seki and Prof. Yuichi Masubuchi for their helpful suggestions as the dissertation committee of this thesis. I also appreciate Associate Prof. Daisuke Kawaguchi of Kyushu University and Assistant Prof. Atsushi Noro for their beneficial comments at seminars.

This study was supported by many researchers in other laboratories. I would like to express my gratitude to Associate Prof. Yoshiaki Takahashi of Kyushu University, Prof. Hiroshi Watanabe of Kyoto University and Prof. Tadashi Inoue of Osaka University for their various discussion and valuable advices, especially on the rheological data. I also appreciate Dr. Jacque Roovers for fruitful discussion and providing rheological data of star polystyrenes. I would thank Associate Prof. Yo Nakamura and Assistant Prof. Daichi Ida of Kyoto University for their beneficial advices, especially on characterization and dilute solution properties of various ring-based polymers. I am thankful to Prof. Masami Kamigaito and Associate Prof. Kotaro Sato of Nagoya University for their help in SEC-MALS measurements. I would also thank Mr. Masahide Nakamura and Mr. Kazuki Watanabe of Shoko Scientific Co. for their help in SEC-MALS-QELS-viscometry measurements.

I would like to thank Prof. Jimmy Mays, Assistant Prof. Namgoo Kang and all of the labmates of the University of Tennessee, and Dr. Kunlun Hong of Oak Ridge National Laboratory for their acceptance of my staying and for providing a precious opportunity.

This work was financially supported by the Program for Leading Graduate Schools at Nagoya University entitled “Integrative Graduate Education and Research Program in Green Natural Sciences” and by JSPS Research Fellowships for Young Scientists (No. 26003393). I would appreciate the above supports.

I am grateful to Dr. Yutaka Ohta and Mr. Kazuki Matsubara for their full supports of this study, especially for preparation and rheological measurements of highly-purified trivial ring polymers. I would like to thank all of the labmates of the Matsushita group for an enjoyable time during the whole of my Ph.D. Finally, I am deeply grateful to my parents for always supporting me.

January, 2016

Yuya Doi